

**SOLUTIONS TO THREE-DIMENSIONAL THIN-LAYER NAVIER-STOKES  
EQUATIONS IN ROTATING COORDINATES FOR FLOW  
THROUGH TURBOMACHINERY**

**By**

**Amrit Raj Ghosh**

**A Thesis  
Submitted to the Faculty of  
Mississippi State University  
in Partial Fulfillment of the Requirements  
for the Degree of Master of Science  
in Aerospace Engineering  
in the Department of Aerospace Engineering**

**Mississippi State, Mississippi**

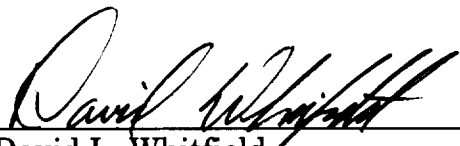
**December 1996**

SOLUTIONS TO THREE-DIMENSIONAL THIN-LAYER NAVIER-STOKES  
EQUATIONS IN ROTATING COORDINATES FOR FLOW  
THROUGH TURBOMACHINERY

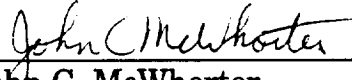
By

Amrit Raj Ghosh

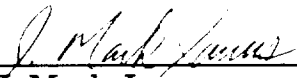
Approved:



David L. Whitfield  
Professor of Aerospace Engineering  
(Director of Thesis)



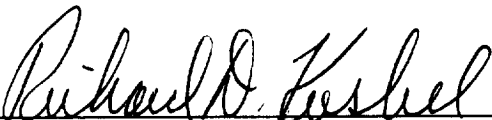
John C. McWhorter  
Graduate Coordinator of the  
Department of Aerospace  
Engineering



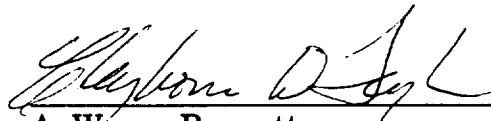
J. Mark Janus  
Assistant Professor of Aerospace  
Engineering  
(Committee Member)



Jen-Ping Chen  
Research Engineer, ERC  
(Committee Member)



Richard D. Koshel  
Dean of the Graduate School



A. Wayne Bennett  
Dean of the College of Engineering

Name: Amrit Raj Ghosh

Date of Degree: December 13, 1996

Institution: Mississippi State University

Major Field: Aerospace Engineering

Major Professor: David L. Whitfield

Title of Study: SOLUTIONS TO THREE-DIMENSIONAL THIN-LAYER  
NAVIER-STOKES EQUATIONS IN ROTATING COORDI-  
NATES FOR FLOW THROUGH TURBOMACHINERY

Pages in Study: 73

Candidate for Degree of Master of Science

The viscous, Navier-Stokes solver for turbomachinery applications, MSUTC has been modified to include the rotating frame formulation. The three-dimensional thin-layer Navier-Stokes equations have been cast in a rotating Cartesian frame enabling the freezing of grid motion. This also allows the flow-field associated with an isolated rotor to be viewed as a steady-state problem. Consequently, local time stepping can be used to accelerate convergence. The formulation is validated by running NASA's Rotor 67 as the test case. Results are compared between the rotating frame code and the absolute frame code. The use of the rotating frame approach greatly enhances the performance of the code with respect to savings in computing time, without degradation of the solution.

## DEDICATION

This thesis is dedicated to my parents, Nirmalendu and Krishna Ghosh, and to the everlasting memory of my grandmother, Shanti Lata Bose.

## ACKNOWLEDGEMENTS

I would like to take this opportunity to express my sincere appreciation and deep sense of gratitude to Dr. David Whitfield for introducing me to the field of CFD, his teaching, and his patience, understanding, and guidance throughout the course of this work. Thanks to Dr. Mark Janus for being on my committee.

A special thank you to Dr. Jen Ping Chen for the guidance he provided throughout this work, for painstakingly answering all my questions and queries and for being on my committee. I am also grateful to Dr. Lafe Taylor and Dr. Abi Arabshahi for getting me over the initial hang-up of understanding and running a 3-D CFD code. I also thank Dr. Murali Beddhu for reading my thesis and making valuable suggestions and clearing a lot of my doubts about the confusion of reference frames. I am grateful to Dr. Z.U.A. Warsi for introducing me to the field of tensors and removing my fear of superscripts and subscripts.

I would like to extend my warmest thanks to all my friends for making my stay here, one of the most memorable phases in my life. Sreenivas, 'the answer guy', for helping everytime I went and cried to him about anything. Shyam, Rajeev, and Rambabu for their support, encouragement and advise. Laxman, for being a good friend and helping me out in my time of crisis. Pradeep 'Bhaisaab' and Bhabhiji for providing me with food and shelter and for always boosting my spirits when I was going through trying times. Ramesh, for his jibes about my graduation. Gayatri, Vikram and Minnie for all those nice parties. And to Rao,

Goyalia, Krishnaraj, Sanjay, Gill, Aditya, Edward, ND, Rahul, Lokesh, Rizwan, Dilnaz, Sudeep and Nivu for all the good times we shared together.

This research was supported by NASA Lewis Research Center under Grant NAG-3-1712, Dr. Eric McFarland, Contract Monitor. Computing time was provided by NSF Engineering Research Center at MSU.

## TABLE OF CONTENTS

	Page
DEDICATION .....	ii
ACKNOWLEDGEMENTS .....	iv
LIST OF TABLES .....	vii
LIST OF FIGURES .....	viii
CHAPTER	
I. INTRODUCTION .....	1
II. GOVERNING EQUATIONS .....	4
2.1 Continuity Equation .....	8
2.2 Momentum Equation .....	8
2.3 Energy Equation .....	9
2.4 Conservation Law Vector form of the Equations .....	9
2.5 Non-Dimensionalization of the Equations .....	13
2.6 Curvilinear Coordinate Transformation .....	14
2.6.1 Thin-Layer Approximation .....	19
III. NUMERICAL SOLUTION METHOD .....	22
3.1 Finite Volume Discretization .....	22
3.2 Implicit Formulation .....	23
3.3 Newton's Formulation .....	24
3.3.1 Flux Vector Splitting .....	26
3.3.2 Viscous Flux Jacobian .....	27
3.4 Flux Formulation .....	28
3.4.1 Convective Flux Computation .....	28

CHAPTER	Page
3.4.2 Diffusive Flux Computation .....	29
3.4.3 Turbulence Modeling .....	30
3.5 The N-Pass Scheme .....	31
3.6 Boundary Conditions .....	32
3.6.1 Subsonic Outflow .....	32
IV. RESULTS .....	37
4.1 Rotor 67 .....	37
V. SUMMARY AND CONCLUSIONS .....	55
REFERENCES .....	57
 APPENDIX	
A. DERIVATION OF THE VELOCITY OF THE MOVING COORDINATES .....	59
B. CURVILINEAR COORDINATE TRANSFORMATION OF THE NAVIER-STOKES EQUATIONS .....	62
C. CYLINDRICAL COORDINATE FORMULATION .....	68



## LIST OF TABLES

TABLE		Page
4.1	Performance Enhancement .....	40

## LIST OF FIGURES

FIGURE		Page
2.1	Rotating Cartesian Coordinate Frame .....	6
3.1	Unit Volume Computational Cell .....	22
3.2	Codirectional Outflow .....	33
4.1	Mass Flow History (back pr. = 0.75) .....	43
4.2	Mass Flow History (log-linear, back pr. = 0.75) .....	43
4.3	Mass Flow History (back pr. = 0.85) .....	44
4.4	Mass Flow History (log-linear, back pr. = 0.85) .....	44
4.5	Mass Flow History (back pr. = 0.90) .....	45
4.6	Mass Flow History (log-linear, back pr. = 0.90) .....	45
4.7	Mass Flow Ratio History (back pr. = 0.75) .....	46
4.8	Mass Flow Ratio History (log-linear, back pr. = 0.75) .....	46
4.9	Mass Flow Ratio History (back pr. = 0.85) .....	47
4.10	Mass Flow Ratio History (log-linear, back pr. = 0.85) .....	47
4.11	Mass Flow Ratio History (back pr. = 0.90) .....	48
4.12	Mass Flow Ratio History (log-linear, back pr. = 0.90) .....	48
4.13	Relative Mach No. Contours at 10% Span for Near Peak Efficiency .....	49
4.14	Relative Mach No. Contours at 30% Span for Near Peak Efficiency .....	50

FIGURE		Page
4.15	Relative Mach No. Contours at 70% Span for Near Peak Efficiency .....	51
4.16	Relative Mach No. Contours at 10% Span for Near Stall .....	52
4.17	Relative Mach No. Contours at 30% Span for Near Stall .....	53
4.18	Relative Mach No. Contours at 70% Span for Near Stall .....	54
A.1	Plane of Rotation .....	60

## CHAPTER I

### INTRODUCTION

The flow field associated with turbomachinery applications is very complex. This flow field is highly unsteady, involving a wide range of time and length scales [1]. The goal of a CFD code for simulating such flows is to be able to model all aspects of the flow phenomena reasonably well. The computing time that is required should also be practically feasible for the CFD code to be useful as a design tool for turbomachinery applications.

The MSUTC code, which is a turbomachinery flow analysis research tool, is an attempt to achieve this goal. This code has been under development at the NSF ERC for Computational Field Simulation at Mississippi State University. It is a viscous flow solver which is capable of simulating even or uneven-blade-count, single-rotating, counter-rotating or rotor-stator, axisymmetric or non-symmetric, multistage, at angle-of attack geometries. Chen [2] noted that though converged unsteady solutions can be obtained using the above code, they are very expensive, because the use of Newton sub-iterations requires tremendous computing time. Thus, the performance of the code can be enhanced if one can avoid the Newton sub-iterations.

Navier-Stokes equations which are the governing equations of fluid mechanics can be expressed in the vector invariant form so that they are independent of the coordinate system. For flows in rotating machinery, it is convenient to cast the equations in the rotating coordinate system. Adamczyk et al. [3] cast

the equations in a rotating cylindrical coordinate system to simulate viscous flow through turbines. Although unsteady computations are very important in turbomachinery simulation, many of the problems can be viewed as steady-state problems in the rotating frame, e.g. an isolated rotor. Consequently, local time stepping and multigrid methods can be utilized to accelerate convergence.

Due to this motivation, at the start of this study an effort was made to develop a cylindrical coordinate system Navier-Stokes code for simulating the steady flow through a single blade row machine. During the course of the investigation it was realized that only a few modifications were necessary to incorporate the rotating frame formulation into the existing unsteady code if one retained the Cartesian coordinate system but solved the problem in a rotating frame similar to the approach in [4] and [5]. This is the approach that was adopted for the work presented in this study. The existing viscous solver is modified to include the rotating frame formulation using the absolute velocity vector.

This thesis is divided into five chapters. Chapter II develops the governing equations cast in the rotating Cartesian coordinate frame. The velocity used in the equations, however is the absolute velocity represented in the rotating frame. The equations are then non-dimensionalized and transformed from Cartesian coordinates to steady curvilinear coordinates to enable the use of a body conforming grid. The thin layer approximation is also explained in this chapter. Chapter III describes the aspects of the flow solver with all the changes that are made due to the change in the formulation. The implicit formulation, Newton's method, flux formulation, flux Jacobians, the N-Pass solution scheme and the boundary conditions are all explained and discussed in this chapter. Chapter IV

presents the results obtained from the modified code. The test case used is NASA's Rotor 67. The results obtained from the rotating frame approach are compared with those obtained from the absolute frame approach. Chapter V is devoted to summary and conclusions.

## CHAPTER II

### GOVERNING EQUATIONS

The development of the Navier-Stokes equations in the rotating coordinates are presented in this chapter. The primary objective in this study is to make use of the quantities in the fixed frame formulation so that a minimum amount of changes need to be made to the existing code. To achieve this goal, the formulation presented in this chapter develops the Navier-Stokes equations in rotating coordinates using the absolute velocity, i.e. velocity with respect to the fixed inertial frame.

The differential forms of the equations of conservation of mass, momentum and energy can be collectively stated in a general form. The differential form of the general conservation principle can be stated as [6]:

$$\frac{\partial \tilde{A}}{\partial t} + \operatorname{div} \tilde{f} = \tilde{C} \quad (2.1)$$

where  $\tilde{f} = \tilde{A}\tilde{u} + \tilde{B}$  and  $\tilde{A}$ ,  $\tilde{B}$ ,  $\tilde{C}$ , are tensor quantities such that  $\tilde{A}$  and  $\tilde{C}$  have the same tensorial order, and if  $\tilde{B} \neq 0$  then it is an order higher than  $\tilde{A}$  and  $\tilde{C}$ . Equation (2.1) is written with respect to an inertial frame so that the vector  $\tilde{u}$  is the absolute velocity. Consider a transformation from the inertial frame to a moving non-inertial frame which is of the form [6]:

$$x^i = x^i(x_1, x_2, x_3, t), \quad i = 1, 2, 3 \quad \text{and} \quad \tau = t$$

where  $(x_1, x_2, x_3)$  are the rectangular Cartesian coordinates defining the somehow, inertial frame.  $(x^1, x^2, x^3)$  are the general coordinates defining the moving frame and  $\underline{a}_{\sim i}$  are the covariant base vectors of the moving frame. If the relative velocity of a fluid particle, which is the velocity with respect to the nonsteady coordinates, is denoted by  $\underline{v}$  and the velocity of the moving coordinates is denoted by  $\underline{w}$ ; the absolute velocity of a fluid particle can be expressed by the following equation [6]:

$$\underline{u} = \underline{v} - \underline{w} \quad (2.2)$$

where

$$\underline{w} = \frac{\partial x^i}{\partial t} \underline{a}_{\sim i} \quad (2.3)$$

The contravariant components of  $\underline{w}$  are the partial time derivatives of each of the coordinates in the moving frame and it can be proven to be negative of the velocity of the moving frame with respect to the inertial frame. Thus, the vector  $\underline{w}$  can be thought of as the velocity of the absolute frame, which an observer in the rotating frame would notice. Details of the derivation are presented in Appendix A.

Due to the above transformation, the following relation exists between the partial time derivatives in the two frames of reference [6]:

$$\frac{\partial(\ )}{\partial t} = \frac{\partial(\ )}{\partial \tau} + \underline{w} \cdot \text{grad}(\ ) \quad (2.4)$$

Thus, the unified conservation law, equation (2.1), transforms to [6]:



$$\frac{\partial \tilde{A}}{\partial \tau} + (\text{grad } \tilde{A}) \cdot \tilde{w} + \text{div } \tilde{f} = \tilde{C} \quad (2.5)$$

The rotating Cartesian coordinate frame utilized in this study is illustrated below.

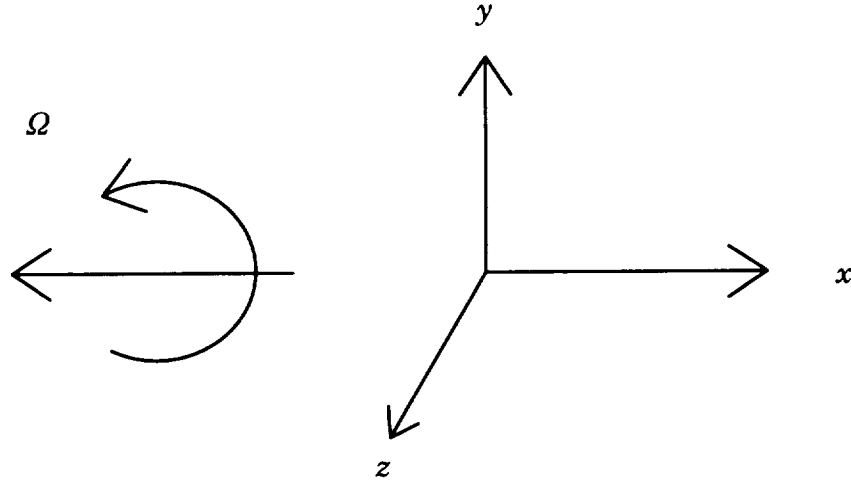


Figure 2.1 Rotating Cartesian Coordinate Frame

It is evident from Figure 2.1 that the rotating frame is rectangular Cartesian in nature, due to which there is no distinction between covariant and contravariant components. Also the base vectors do not vary in space, so that:

$$\frac{\partial a_{\tilde{j}}}{\partial x^i} = 0 \quad (2.6)$$

The temporal derivatives of the base vectors are given by [6]:

$$\frac{\partial a_{\tilde{i}}}{\partial \tau} + \frac{\partial w_{\tilde{i}}}{\partial x^i} = 0 \quad (2.7)$$

Choosing a rotating frame illustrated in Figure 2.1 results in:  $\tilde{w} = -\tilde{\Omega} \times \tilde{r}$

where  $\tilde{\Omega} = -\Omega a_{\tilde{1}}$ . Therefore,  $\tilde{w} = -\Omega x^3 a_{\tilde{2}} + \Omega x^2 a_{\tilde{3}}$ . Consequently,

$$\operatorname{div} \underline{\underline{w}} = \frac{\partial w}{\partial x^i} \cdot \underline{\underline{a}}^i = \frac{\partial w^j}{\partial x^i} \underline{\underline{a}}_j \cdot \underline{\underline{a}}^i = \frac{\partial w^i}{\partial x^i} = 0 \quad (2.8)$$

Using the following tensor identity :

$$\operatorname{div} (\underline{\underline{A}}\underline{\underline{w}}) = (\operatorname{grad} \underline{\underline{A}}) \cdot \underline{\underline{w}} + (\operatorname{div} \underline{\underline{w}})\underline{\underline{A}} = (\operatorname{grad} \underline{\underline{A}}) \cdot \underline{\underline{w}} \quad (2.9)$$

and equation (2.8), one can rewrite equation (2.5) as:

$$\frac{\partial \underline{\underline{A}}}{\partial \tau} + \operatorname{div} (\underline{\underline{A}}\underline{\underline{w}}) + \operatorname{div} \underline{\underline{f}} = \underline{\underline{C}} \quad (2.10)$$

As explained at the beginning of this chapter, the primary objective is to cast the Navier-Stokes equation in the rotating frame using the absolute velocity vector. The continuity, momentum and energy equations that are derived below in this chapter, have used the absolute velocity vector  $\underline{\underline{u}}$ . However, all the vectors appearing in equation (2.10) are represented using the base vectors of the rotating frame. This concept can appear confusing. This confusion is removed by addressing two important aspects related to any velocity vector in the above equations. The first being definition of the vector, and the second is representation of the vector.

The keywords to defining a velocity vector are: *with respect to*. This clarifies which reference frame one is referring to when defining the velocity vector. Thus, the absolute velocity  $\underline{\underline{u}}$ , is defined as the velocity of a fluid particle in the concerned flowfield, *with respect to* the fixed inertial frame. Therefore, a stationary observer who selects a right handed rectangular coordinate system like the one in Figure 2.1, but one which is not moving, observes the velocity of a fluid particle in the flow field as  $\underline{\underline{u}}$ . On the other hand, an observer moving with the

axes described in Figure 2.1, observes the velocity of the fluid particle in the flow field as  $\underline{v}$ . Thus, the relative velocity  $\underline{v}$ , is defined as the velocity of a fluid particle *with respect to* the rotating non-inertial reference frame.

Once the definition of the vector is taken care of, the issue of representing the vector arises. These two issues are independent of each other and once a vector is defined *with respect to* a frame, there is no need to express the components of the same vector using a coordinate system in the same frame. Thus, the absolute velocity vector can be expressed in component form with respect to the basis of the rotating Cartesian coordinate system shown in Figure 2.1. Since the exercise in this chapter is to cast the Navier-Stokes equations in the rotating frame, all the mathematical operations arising in the equations below, viz., time derivatives, curl, grad, div, are carried out in the rotating frame and involve its base vectors. To be consistent and to simplify mathematical operations, the rotating frame has been chosen to represent all vectors and tensors.

### 2.1 Continuity Equation

The continuity equation is obtained from the generalized conservation law, equation (2.10), by substituting  $\tilde{A} = \rho$ ,  $\tilde{f} = \rho \underline{u}$ ,  $\tilde{B} = 0$ ,  $\tilde{C} = 0$ . Thus, the continuity equation in the rotating frame can be written as:

$$\frac{\partial \rho}{\partial \tau} + \text{div}(\rho \underline{w}) + \text{div}(\rho \underline{u}) = 0 \quad (2.11)$$

### 2.2 Momentum Equation

The momentum equation in the non-inertial frame is obtained by substituting  $\tilde{A} = \rho \underline{u}$ ,  $\tilde{B} = -\tilde{T} = p\tilde{I} - \tilde{\sigma}$ ,  $\tilde{C} = 0$  in equation (2.10).

The resulting equation is:

$$\frac{\partial(\rho u)}{\partial \tau} + \text{div}(\rho u w) + \text{div}(\rho u u) = \text{div}(\tilde{T}) \quad (2.12)$$

where  $\tilde{T}$  is the stress tensor,  $p$  is the thermodynamic static pressure,  $\tilde{I}$  is the identity tensor and  $\tilde{\sigma}$  is the deviatoric part of the stress tensor containing the viscous shear stress. It can be represented by:

$$\tilde{\sigma} = \lambda(\text{div } \underline{u})\tilde{I} + \mu[(\text{grad } \underline{u}) + (\text{grad } \underline{u})^T] \quad (2.13)$$

where  $\mu$  and  $\lambda$  are the first and second coefficients of viscosity, respectively. Writing  $\underline{u} = u^i \underline{a}_i$  and utilizing the result in equation (2.7), the momentum equation can be rewritten as:

$$\frac{\partial(\rho u^i)}{\partial \tau} \underline{a}_i + \text{div}(\rho u w) + \text{div}(\rho u u) = \text{div}(\tilde{T}) + \rho u^i \frac{\partial w}{\partial x^i} \quad (2.14)$$

### 2.3 Energy Equation

The generalized conservation law, equation (2.10), yields the energy equation by substituting  $\tilde{A} = e_t$ ,  $\tilde{B} = -\tilde{T} \cdot \underline{u} + \underline{q}$ ,  $\tilde{C} = 0$ , where

$e_t = \frac{p}{\gamma-1} + \frac{1}{2}\rho |\underline{u}|^2$  is the total energy and  $\underline{q}$  is the conductive heat flux vector.

The energy equation in the rotating frame, therefore, is:

$$\frac{\partial e_t}{\partial \tau} + \text{div}(e_t w) + \text{div}(e_t u) = \text{div}(\tilde{T} \cdot \underline{u}) - \text{div}(\underline{q}) \quad (2.15)$$

### 2.4 Conservation Law Vector form of the Equations

Equations (2.11), (2.14) and (2.15) can be expanded and written in the

conservation law form by carrying out the mathematical operations of divergence and dot products on the various vectors and tensors involved. While doing the operations involving the base vectors one utilizes the results that the base vectors do not vary in space and that since the coordinate axes are rectangular Cartesian in nature;  $\underline{a}_i \cdot \underline{a}_j = \delta_{ij}$ . For simplicity, let  $x^1 = x$ ,  $x^2 = y$ ,  $x^3 = z$ ,  $\tau = t$  and  $u^1 = u$ ,  $u^2 = v$ ,  $u^3 = w$ . The five equations that result can then be combined into one single vector equation of the form:

$$\frac{\partial q}{\partial t} + \frac{\partial f}{\partial x} + \frac{\partial g}{\partial y} + \frac{\partial h}{\partial z} = \frac{\partial f^v}{\partial x} + \frac{\partial g^v}{\partial y} + \frac{\partial h^v}{\partial z} + s \quad (2.16)$$

where the dependent variable vector  $q$ , the flux vectors  $f$ ,  $g$ ,  $h$ , the viscous flux vectors  $f^v$ ,  $h^v$ ,  $g^v$ , and the source term vector  $s$  are defined as follows:

$$q = \begin{bmatrix} \rho \\ \rho u \\ \rho v \\ \rho w \\ e_t \end{bmatrix} \quad (2.17)$$

$$f = \begin{bmatrix} \rho u \\ \rho u^2 + p \\ \rho uv \\ \rho uw \\ u(e_t + p) \end{bmatrix}, \quad g = \begin{bmatrix} \rho v - \rho \Omega z \\ \rho vu - \rho u \Omega z \\ \rho v^2 + p - \rho v \Omega z \\ \rho vw - \rho w \Omega z \\ v(e_t + p) - e_t \Omega z \end{bmatrix}, \quad h = \begin{bmatrix} \rho w + \rho \Omega y \\ \rho wu + \rho u \Omega y \\ \rho wv + \rho v \Omega y \\ \rho w^2 + p + \rho w \Omega y \\ w(e_t + p) + e_t \Omega y \end{bmatrix} \quad (2.18)$$

$$f^v = \begin{bmatrix} 0 \\ \tau_{xx} \\ \tau_{xy} \\ \tau_{xz} \\ u\tau_{xx} + v\tau_{xy} + w\tau_{xz} + q_x \end{bmatrix}$$

$$g^v = \begin{bmatrix} 0 \\ \tau_{yx} \\ \tau_{yy} \\ \tau_{yz} \\ u\tau_{yx} + v\tau_{yy} + w\tau_{yz} + q_y \end{bmatrix} \quad (2.19)$$

$$h^v = \begin{bmatrix} 0 \\ \tau_{zx} \\ \tau_{zy} \\ \tau_{zz} \\ u\tau_{zx} + v\tau_{zy} + w\tau_{zz} + q_z \end{bmatrix}$$

$$s = \begin{bmatrix} 0 \\ 0 \\ -\rho w \Omega \\ \rho v \Omega \\ 0 \end{bmatrix} \quad (2.20)$$

The viscous stress terms appearing in the equation (2.19) are defined below under the assumption that bulk viscosity is negligible, so that  $\lambda = -\frac{2}{3}\mu$ .

$$\begin{aligned} \tau_{xx} &= \frac{2}{3}\mu\left(2\frac{\partial u}{\partial x} - \frac{\partial v}{\partial y} - \frac{\partial w}{\partial z}\right), & \tau_{xy} &= \tau_{yx} = \mu\left(\frac{\partial u}{\partial y} + \frac{\partial v}{\partial x}\right) \\ \tau_{yy} &= \frac{2}{3}\mu\left(2\frac{\partial v}{\partial y} - \frac{\partial u}{\partial x} - \frac{\partial w}{\partial z}\right), & \tau_{yz} &= \tau_{zy} = \mu\left(\frac{\partial v}{\partial z} + \frac{\partial w}{\partial y}\right) \\ \tau_{zz} &= \frac{2}{3}\mu\left(2\frac{\partial w}{\partial z} - \frac{\partial u}{\partial x} - \frac{\partial v}{\partial y}\right), & \tau_{zx} &= \tau_{xz} = \mu\left(\frac{\partial w}{\partial x} + \frac{\partial u}{\partial z}\right) \end{aligned} \quad (2.21)$$

The conductive heat flux terms which appear in the viscous flux vectors are defined below. The conductive heat flux vector is defined as:  $\underline{q} = -k(\text{grad } T)$  where  $k$  is the thermal conductivity, and  $T$  is the temperature. The components of the heat flux vectors along each of the coordinate directions, therefore, are:

$$\begin{aligned}
q_x &= k \frac{\partial T}{\partial x} \\
q_y &= k \frac{\partial T}{\partial y} \\
q_z &= k \frac{\partial T}{\partial z}
\end{aligned}
\tag{2.22}$$

All the components of the tensors and vectors that appeared in the equation (2.16) are in terms of the base vectors of the rotating frame. The existing code uses a fixed frame formulation so that the components involved are in terms of the base vectors of the fixed frame. For the purpose of validation of the rotating frame formulation one needs to be able to compare the flow fields generated as the solutions from the two formulations. Thus, a relation between components in the rotating frame and components in the fixed frame needs to be obtained. Letting  $u_a$ ,  $v_a$ , and  $w_a$  be the components of the absolute velocity with respect to a Cartesian coordinate system in the fixed frame, and, assuming for convenience, that the initial configuration of the rotating frame matches with the stationary frame (say at instant  $t = 0$ ); the following relations are obtained:

$$\begin{aligned}
u_a &= u \\
v_a &= v \cos(\Omega t) - w \sin(\Omega t) \\
w_a &= v \sin(\Omega t) + w \cos(\Omega t)
\end{aligned}
\tag{2.23}$$

where, it is emphasized that  $u$ ,  $v$ , and  $w$  are the components of the absolute velocity with respect to a rotating Cartesian basis. It is apparent from the above equation that at instant  $t = 0$  and after every subsequent full rotation, the components of the absolute velocity in the rotating frame are identical to the components in the stationary frame.

Now, the Navier-Stokes equations have already been cast in the moving frame, so that there is no need to move the grid anymore. The flow field that is

generated in terms of the components, by solving the Navier-Stokes equations in the form presented in equation (2.16), for purposes of comparison, can be changed according to equation (2.23) to match the flow field which results from solving Navier-Stokes equations derived in the inertial frame. However, the distinct advantage of the former over the latter is that local time stepping can be used for steady flows in the rotating frame. Another advantage is the freezing of grid motion because in the fixed frame formulation the grid motion is imperative.

### 2.5 Non-Dimensionalization of the Equations

All the variables used in the formulation till now are dimensional variables. In order to obtain a form of the equation (2.16) with non-dimensional quantities, a scaling of all the dimensional variables (denoted by  $\hat{\cdot}$ ) is carried out using the following relations:

$$\begin{aligned}
 x &= \frac{\hat{x}}{\hat{D}}, & y &= \frac{\hat{y}}{\hat{D}}, & z &= \frac{\hat{z}}{\hat{D}}, & u &= \frac{\hat{u}}{\hat{a}_0}, & v &= \frac{\hat{v}}{\hat{a}_0}, & w &= \frac{\hat{w}}{\hat{a}_0}, & \Omega &= \frac{\hat{D}\hat{\Omega}}{\hat{a}_0} \\
 p &= \frac{\hat{p}}{\hat{\rho}_0\hat{a}_0^2}, & \rho &= \frac{\hat{\rho}}{\hat{\rho}_0}, & t &= \frac{\hat{a}_0\hat{t}}{\hat{D}}, & e &= \frac{\hat{e}}{\hat{\rho}_0\hat{a}_0^2}, & h &= \frac{\hat{h}}{\hat{a}_0^2}, & \mu &= \frac{\hat{\mu}}{\hat{\mu}_0} \\
 \tau_{ij} &= \frac{\hat{\tau}_{ij}}{\hat{\rho}_0\hat{a}_0^2}, & \tau_{wall} &= \frac{\hat{\tau}_{wall}}{\left(\frac{\hat{\mu}_0\hat{a}_0}{\hat{D}}\right)}, & q_{x_i} &= \frac{\hat{q}_{x_i}}{\hat{\rho}_0\hat{a}_0^3}, & T &= \frac{\hat{T}}{\hat{T}_0}, & \hat{a}_0^2 &= \gamma\hat{R}\hat{T}_0
 \end{aligned}$$

The scaling has been accomplished using the reference quantities (denoted by subscript 0) which are the total conditions and the reference length  $\hat{D}$  which is the maximum diameter of the blade tip. The detailed development of the scaling of the equations can be found in [2]. The scaling results in a form of



the vector equation which is exactly similar to equation (2.16) but with non-dimensional variables. The form of the dependent variable, flux, viscous flux and the source term vectors is also exactly same as shown in equations (2.17) - (2.20), but with all variables non-dimensional. The only difference arising out of the scaling of equations is the introduction of two new non-dimensional quantities, viz., Reynolds and Prandtl numbers (Re, Pr), which appear in the non-dimensional form of the viscous shear stress and the conductive heat flux terms. The non-dimensional viscous shear stress and the conductive heat flux terms are:

$$\begin{aligned}
 \tau_{xx} &= \frac{1}{\text{Re}} \frac{2}{3} \mu \left( 2 \frac{\partial u}{\partial x} - \frac{\partial v}{\partial y} - \frac{\partial w}{\partial z} \right), & \tau_{xy} &= \tau_{yx} = \frac{1}{\text{Re}} \mu \left( \frac{\partial u}{\partial y} + \frac{\partial v}{\partial x} \right) \\
 \tau_{yy} &= \frac{1}{\text{Re}} \frac{2}{3} \mu \left( 2 \frac{\partial v}{\partial y} - \frac{\partial u}{\partial x} - \frac{\partial w}{\partial z} \right), & \tau_{yz} &= \tau_{zy} = \frac{1}{\text{Re}} \mu \left( \frac{\partial v}{\partial z} + \frac{\partial w}{\partial y} \right) \\
 \tau_{zz} &= \frac{1}{\text{Re}} \frac{2}{3} \mu \left( 2 \frac{\partial w}{\partial z} - \frac{\partial u}{\partial x} - \frac{\partial v}{\partial y} \right), & \tau_{zx} &= \tau_{xz} = \frac{1}{\text{Re}} \mu \left( \frac{\partial w}{\partial x} + \frac{\partial u}{\partial z} \right)
 \end{aligned} \tag{2.24}$$

$$\begin{aligned}
 q_x &= \frac{1}{\text{Re}} \left[ \frac{\mu}{(\gamma - 1) \text{Pr}} \right] \frac{\partial T}{\partial x} \\
 q_y &= \frac{1}{\text{Re}} \left[ \frac{\mu}{(\gamma - 1) \text{Pr}} \right] \frac{\partial T}{\partial y} \\
 q_z &= \frac{1}{\text{Re}} \left[ \frac{\mu}{(\gamma - 1) \text{Pr}} \right] \frac{\partial T}{\partial z}
 \end{aligned} \tag{2.25}$$

where  $\text{Re} = \frac{\hat{\rho}_0 \hat{a}_0 \hat{D}}{\hat{\mu}_0}$  and  $\text{Pr} = \frac{\hat{c}_p \hat{\mu}}{\hat{k}}$ .

## 2.6 Curvilinear Coordinate Transformation

In order to carry out numerical computation of the governing equations on a configuration comprising of a complex geometry, it is simpler to use a body-conforming grid in which the solid surfaces in the geometry correspond to

constant coordinate surfaces. To this end, a curvilinear coordinate transformation needs to be introduced in the rectangular Cartesian space being used in the formulation thus far. The following general, nonorthogonal, steady, curvilinear coordinate system is introduced in the  $(x, y, z)$  space:

$$\begin{aligned}\xi &= \xi(x, y, z) \\ \eta &= \eta(x, y, z) \\ \zeta &= \zeta(x, y, z) \\ \tau &= t\end{aligned}\tag{2.26}$$

Only the final results due to the transformation are stated in this section. A detailed presentation of all the steps involved and the how the relations for the metric terms are obtained, is made in Appendix B. Using chain rule yields:

$$\begin{aligned}\frac{\partial}{\partial t} &= \frac{\partial}{\partial \tau} \\ \frac{\partial}{\partial x} &= \xi_x \frac{\partial}{\partial \xi} + \eta_x \frac{\partial}{\partial \eta} + \zeta_x \frac{\partial}{\partial \zeta} \\ \frac{\partial}{\partial y} &= \xi_y \frac{\partial}{\partial \xi} + \eta_y \frac{\partial}{\partial \eta} + \zeta_y \frac{\partial}{\partial \zeta} \\ \frac{\partial}{\partial z} &= \xi_z \frac{\partial}{\partial \xi} + \eta_z \frac{\partial}{\partial \eta} + \zeta_z \frac{\partial}{\partial \zeta}\end{aligned}\tag{2.27}$$

The Jacobian  $J$  of the inverse transformation is:

$$\begin{aligned}J &= \det \left| \frac{\partial(x, y, z)}{\partial(\xi, \eta, \zeta)} \right| \\ &= x_\xi(y_\eta z_\zeta - z_\eta y_\zeta) - y_\xi(x_\eta z_\zeta - z_\eta x_\zeta) + z_\xi(x_\eta y_\zeta - y_\eta x_\zeta)\end{aligned}\tag{2.28}$$

The metric terms in equation (2.27) are:

$$\begin{aligned}\xi_x &= \frac{1}{J}(y_\eta z_\zeta - z_\eta y_\zeta) & \eta_x &= \frac{1}{J}(z_\xi y_\zeta - y_\xi z_\zeta) & \zeta_x &= \frac{1}{J}(y_\xi z_\eta - z_\xi y_\eta) \\ \xi_y &= \frac{1}{J}(z_\eta x_\zeta - x_\eta z_\zeta) & \eta_y &= \frac{1}{J}(x_\xi z_\zeta - z_\xi x_\zeta) & \zeta_y &= \frac{1}{J}(z_\xi x_\eta - x_\xi z_\eta) \\ \xi_z &= \frac{1}{J}(x_\eta y_\zeta - y_\eta x_\zeta) & \eta_z &= \frac{1}{J}(y_\xi x_\zeta - x_\xi y_\zeta) & \zeta_z &= \frac{1}{J}(x_\xi y_\eta - y_\xi x_\eta)\end{aligned}\tag{2.29}$$

Substituting relations obtained in equation (2.27) into equation (2.16) results in the form of the governing equations in stationary curvilinear coordinates. Only the final equation is stated here. The resulting form is:

$$\frac{\partial Q}{\partial \tau} + \frac{\partial F}{\partial \xi} + \frac{\partial G}{\partial \eta} + \frac{\partial H}{\partial \zeta} = \frac{\partial F^v}{\partial \xi} + \frac{\partial G^v}{\partial \eta} + \frac{\partial H^v}{\partial \zeta} + S \quad (2.30)$$

where

$$Q = J \begin{bmatrix} \rho \\ \rho u \\ \rho v \\ \rho w \\ e_t \end{bmatrix} \quad (2.31)$$

$$\bar{K} = J \begin{bmatrix} \rho K' \\ \rho u K' + k_x p \\ \rho v K' + k_y p \\ \rho w K' + k_z p \\ e_t K' + p K \end{bmatrix}, \quad \begin{aligned} \text{where } K' &= k_x u + k_y v + k_z w + k_t \\ k_t &= -k_y \Omega z + k_z \Omega y \\ K &= k_x u + k_y v + k_z w \end{aligned} \quad (2.32)$$

$$\bar{K}^v = J \begin{bmatrix} 0 \\ T_{kx} \\ T_{ky} \\ T_{kz} \\ Q_k \end{bmatrix} \quad (2.33)$$

$$S = J \begin{bmatrix} 0 \\ 0 \\ -\rho w \Omega \\ \rho v \Omega \\ 0 \end{bmatrix} \quad (2.34)$$

In the above equations (2.32) and (2.33),  $\bar{K} = F, G, H$ ;  $K' = U', V', W'$ ;  $K = U, V, W$ ;  $\bar{K}^v = F^v, G^v, H^v$ ; for  $k = \xi, \eta, \zeta$  respectively. The appearance of the term  $k_t$  is to account for the divergence terms in equations (2.11),

(2.14), and (2.15) in which the vector  $\underline{w}$  explicitly appears. This can be further explained by considering the continuity equation, the treatment being same for the other equations. The continuity equation can be rewritten as:

$$\frac{\partial \rho}{\partial t} + \text{div} [ \rho(\underline{u} + \underline{w}) ] = 0 \quad (2.35)$$

which in curvilinear coordinates becomes

$$\frac{\partial(J\rho)}{\partial t} + \frac{\partial}{\partial x^k} [ J\rho(\underline{u} + \underline{w}) \cdot \underline{\alpha}^k ] = 0 \quad (2.36)$$

It can be verified that:

$$k_t = \underline{w} \cdot \underline{\alpha}^k \quad (2.37)$$

and

$$K' = (\underline{u} + \underline{w}) \cdot \underline{\alpha}^k \quad (2.38)$$

In the formulation of the continuity equation in the absolute frame the term  $k_t$  appears in a strikingly similar manner and denotes the contravariant component of the grid velocity vector. In the present formulation, however, there is no grid motion involved and  $k_t$  should not be associated with any grid velocity. It is just the contravariant component of the vector,  $\underline{w} = -\underline{\Omega} \times \underline{r}$ . The expressions for transformed shear stress and heat flux terms are as follows:

$$\begin{aligned} T_{kx} &= k_x \tau_{xx} + k_y \tau_{yx} + k_z \tau_{zx} \\ T_{ky} &= k_x \tau_{xy} + k_y \tau_{yy} + k_z \tau_{zy} \\ T_{kz} &= k_x \tau_{xz} + k_y \tau_{yz} + k_z \tau_{zz} \\ Q_k &= uT_{kx} + vT_{ky} + wT_{kz} + k_x q_x + k_y q_y + k_z q_z \end{aligned} \quad (2.39)$$

where

$$\begin{aligned}
\tau_{xx} &= \frac{1}{\text{Re}} \frac{2}{3} \mu \left[ 2(\xi_x \frac{\partial u}{\partial \xi} + \eta_x \frac{\partial u}{\partial \eta} + \zeta_x \frac{\partial u}{\partial \zeta}) - (\xi_y \frac{\partial v}{\partial \xi} + \eta_y \frac{\partial v}{\partial \eta} + \zeta_y \frac{\partial v}{\partial \zeta}) - \right. \\
&\quad \left. (\xi_z \frac{\partial w}{\partial \xi} + \eta_z \frac{\partial w}{\partial \eta} + \zeta_z \frac{\partial w}{\partial \zeta}) \right] \\
\tau_{yy} &= \frac{1}{\text{Re}} \frac{2}{3} \mu \left[ 2(\xi_y \frac{\partial v}{\partial \xi} + \eta_y \frac{\partial v}{\partial \eta} + \zeta_y \frac{\partial v}{\partial \zeta}) - (\xi_x \frac{\partial u}{\partial \xi} + \eta_x \frac{\partial u}{\partial \eta} + \zeta_x \frac{\partial u}{\partial \zeta}) - \right. \\
&\quad \left. (\xi_z \frac{\partial w}{\partial \xi} + \eta_z \frac{\partial w}{\partial \eta} + \zeta_z \frac{\partial w}{\partial \zeta}) \right] \\
\tau_{zz} &= \frac{1}{\text{Re}} \frac{2}{3} \mu \left[ 2(\xi_z \frac{\partial w}{\partial \xi} + \eta_z \frac{\partial w}{\partial \eta} + \zeta_z \frac{\partial w}{\partial \zeta}) - (\xi_x \frac{\partial u}{\partial \xi} + \eta_x \frac{\partial u}{\partial \eta} + \zeta_x \frac{\partial u}{\partial \zeta}) - \right. \\
&\quad \left. (\xi_y \frac{\partial v}{\partial \xi} + \eta_y \frac{\partial v}{\partial \eta} + \zeta_y \frac{\partial v}{\partial \zeta}) \right] \tag{2.40}
\end{aligned}$$

$$\tau_{xy} = \tau_{yx} = \frac{1}{\text{Re}} \mu \left[ (\xi_y \frac{\partial u}{\partial \xi} + \eta_y \frac{\partial u}{\partial \eta} + \zeta_y \frac{\partial u}{\partial \zeta}) + (\xi_x \frac{\partial v}{\partial \xi} + \eta_x \frac{\partial v}{\partial \eta} + \zeta_x \frac{\partial v}{\partial \zeta}) \right]$$

$$\tau_{yz} = \tau_{zy} = \frac{1}{\text{Re}} \mu \left[ (\xi_z \frac{\partial v}{\partial \xi} + \eta_z \frac{\partial v}{\partial \eta} + \zeta_z \frac{\partial v}{\partial \zeta}) + (\xi_y \frac{\partial w}{\partial \xi} + \eta_y \frac{\partial w}{\partial \eta} + \zeta_y \frac{\partial w}{\partial \zeta}) \right]$$

$$\tau_{zx} = \tau_{xz} = \frac{1}{\text{Re}} \mu \left[ (\xi_x \frac{\partial w}{\partial \xi} + \eta_x \frac{\partial w}{\partial \eta} + \zeta_x \frac{\partial w}{\partial \zeta}) + (\xi_z \frac{\partial u}{\partial \xi} + \eta_z \frac{\partial u}{\partial \eta} + \zeta_z \frac{\partial u}{\partial \zeta}) \right]$$

$$\begin{aligned}
q_x &= \frac{1}{\text{Re}} \left[ \frac{\mu}{(\gamma - 1) \text{Pr}} \right] (\xi_x \frac{\partial T}{\partial \xi} + \eta_x \frac{\partial T}{\partial \eta} + \zeta_x \frac{\partial T}{\partial \zeta}) \\
q_y &= \frac{1}{\text{Re}} \left[ \frac{\mu}{(\gamma - 1) \text{Pr}} \right] (\xi_y \frac{\partial T}{\partial \xi} + \eta_y \frac{\partial T}{\partial \eta} + \zeta_y \frac{\partial T}{\partial \zeta}) \\
q_z &= \frac{1}{\text{Re}} \left[ \frac{\mu}{(\gamma - 1) \text{Pr}} \right] (\xi_z \frac{\partial T}{\partial \xi} + \eta_z \frac{\partial T}{\partial \eta} + \zeta_z \frac{\partial T}{\partial \zeta}) \tag{2.41}
\end{aligned}$$

### 2.6.1 Thin-Layer Approximation

Since the numerical simulation of the full Navier-Stokes equations are very computationally intensive, the thin-layer approximation is used in this study. This approach is useful because it can handle flows which have both inviscid and viscous regions and interactions between the two [2]. The thin-layer approximation makes use of the fact that most grids for Navier-Stokes equations are packed in the direction normal to the walls, whereas along the streamwise direction they are usually very coarse and good enough for inviscid calculations only [2]. In this study,  $\xi$  is the streamwise,  $\eta$  the spanwise, and  $\zeta$  the pitchwise directions. Thus, all the viscous and heat flux derivatives in the streamwise direction are dropped. In the other two directions, only the normal second derivatives are considered while the mixed derivatives are neglected. This is done because they are insignificant in corners and lead to expensive calculations [2]. Applying the above approximation to equation (2.30) gives the following final form of the governing equations:

$$\frac{\partial Q}{\partial \tau} + \frac{\partial F}{\partial \xi} + \frac{\partial G}{\partial \eta} + \frac{\partial H}{\partial \zeta} = \frac{\partial G_v}{\partial \eta} + \frac{\partial H_v}{\partial \zeta} + S \quad (2.42)$$

where

$$Q = J \begin{bmatrix} \rho \\ \rho u \\ \rho v \\ \rho w \\ e_t \end{bmatrix} \quad (2.43)$$

$$F = J \begin{bmatrix} \rho U' \\ \rho u U' + \xi_x p \\ \rho v U' + \xi_y p \\ \rho w U' + \xi_z p \\ e_t U' + p U \end{bmatrix}, \quad G = J \begin{bmatrix} \rho V' \\ \rho u V' + \eta_x p \\ \rho v V' + \eta_y p \\ \rho w V' + \eta_z p \\ e_t V' + p V \end{bmatrix}, \quad H = J \begin{bmatrix} \rho W' \\ \rho u W' + \zeta_x p \\ \rho v W' + \zeta_y p \\ \rho w W' + \zeta_z p \\ e_t W' + p W \end{bmatrix} \quad (2.44)$$

$$G^v = J \begin{bmatrix} 0 \\ T_{\eta x} \\ T_{\eta y} \\ T_{\eta z} \\ Q_\eta \end{bmatrix}, \quad H^v = J \begin{bmatrix} 0 \\ T_{\zeta x} \\ T_{\zeta y} \\ T_{\zeta z} \\ Q_\zeta \end{bmatrix} \quad (2.45)$$

$$S = J \begin{bmatrix} 0 \\ 0 \\ -\rho w \Omega \\ \rho v \Omega \\ 0 \end{bmatrix} \quad (2.46)$$

The terms  $U'$ ,  $V'$ ,  $W'$ , and  $U$ ,  $V$ ,  $W$  are defined in equation (2.32). The expressions for the transformed shear stress and the transformed heat flux terms appearing in the viscous flux vectors are:

$$\begin{aligned} T_{kx} &= k_x \tau_{xx} + k_y \tau_{yx} + k_z \tau_{zx} \\ T_{ky} &= k_x \tau_{xy} + k_y \tau_{yy} + k_z \tau_{zy} \\ T_{kz} &= k_x \tau_{xz} + k_y \tau_{yz} + k_z \tau_{zz} \\ Q_k &= uT_{kx} + vT_{ky} + wT_{kz} + k_x q_x + k_y q_y + k_z q_z \end{aligned} \quad (2.47)$$

In the equation (2.47) above,  $k = \eta, \zeta$  for flux vectors  $G^v, H^v$  respectively. Applying the thin-layer approximation in the  $k$  direction the viscous stress and the conductive heat flux terms will become:

$$\begin{aligned} \tau_{xx} &= \frac{1}{\text{Re}} \frac{2}{3} \mu \left[ 2k_x \frac{\partial u}{\partial k} - k_y \frac{\partial v}{\partial k} - k_z \frac{\partial w}{\partial k} \right] \\ \tau_{yy} &= \frac{1}{\text{Re}} \frac{2}{3} \mu \left[ 2k_y \frac{\partial v}{\partial k} - k_x \frac{\partial u}{\partial k} - k_z \frac{\partial w}{\partial k} \right] \\ \tau_{zz} &= \frac{1}{\text{Re}} \frac{2}{3} \mu \left[ 2k_z \frac{\partial w}{\partial k} - k_x \frac{\partial u}{\partial k} - k_y \frac{\partial v}{\partial k} \right] \end{aligned} \quad (2.48)$$

$$\begin{aligned}
\tau_{xy} = \tau_{yx} &= \frac{1}{\text{Re}} \mu \left[ k_y \frac{\partial u}{\partial k} + k_x \frac{\partial v}{\partial k} \right] \\
\tau_{yz} = \tau_{zy} &= \frac{1}{\text{Re}} \mu \left[ k_z \frac{\partial v}{\partial k} + k_y \frac{\partial w}{\partial k} \right] \\
\tau_{zx} = \tau_{xz} &= \frac{1}{\text{Re}} \mu \left[ k_x \frac{\partial w}{\partial k} + k_z \frac{\partial u}{\partial k} \right]
\end{aligned} \tag{2.49}$$

$$\begin{aligned}
q_x &= \frac{1}{\text{Re}} \left[ \frac{\mu}{(\gamma - 1) \text{Pr}} \right] \left( k_x \frac{\partial T}{\partial k} \right) \\
q_y &= \frac{1}{\text{Re}} \left[ \frac{\mu}{(\gamma - 1) \text{Pr}} \right] \left( k_y \frac{\partial T}{\partial k} \right) \\
q_z &= \frac{1}{\text{Re}} \left[ \frac{\mu}{(\gamma - 1) \text{Pr}} \right] \left( k_z \frac{\partial T}{\partial k} \right)
\end{aligned} \tag{2.50}$$

The approach described in this chapter for the development of the governing equations was not initially employed for this study. The initial route taken was via the cylindrical coordinates. However, it was later realized that the approach described above is much more elegant and less time consuming. It also entails the minimum amount of changes to the existing code for it to work for this particular formulation.

For completeness, the development of the governing equations using cylindrical coordinates in a rotating frame is presented in Appendix C. The final form of the equations derived in Appendix C are then transformed from cylindrical to Cartesian coordinates to see if they match the governing equations derived here in this chapter.



CHAPTER III  
NUMERICAL SOLUTION METHOD

The finite volume approach is utilized to obtain the numerical solution of the thin-layer Navier-Stokes equations which were derived in the previous chapter and are presented in their final form in equation (2.42).

3.1 Finite Volume Discretization

The curvilinear coordinate transformation maps the entire physical domain to a computational domain which is discretized into collection of cells of unit volume. Thus,  $\Delta\xi = \Delta\eta = \Delta\zeta = 1$ . The finite volume formulation is obtained by integrating equation (2.42) over a unit volume computational cell, which is shown in the figure below.

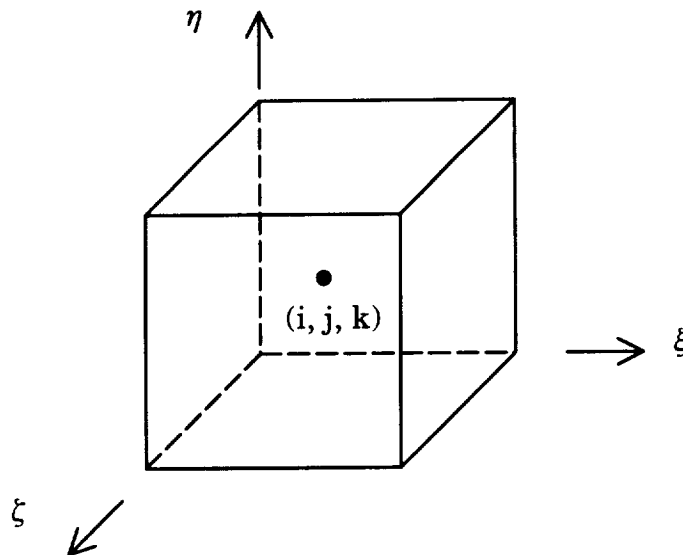


Figure 3.1 Unit Volume Computational Cell

In the cell-centered finite volume approach the dependent variable vector  $Q$ , is assumed to be the flow quantities at the cell center, and is uniform throughout the cell. The fluxes  $F$ ,  $G$ ,  $H$ ,  $G^v$ ,  $H^v$  are assumed to be uniform over each corresponding cell face. The integral form of equation (2.42) after spatial discretization, can then be written as:

$$\begin{aligned} \frac{\partial Q}{\partial \tau} \Delta \xi \Delta \eta \Delta \zeta + (F_{i+\frac{1}{2}} - F_{i-\frac{1}{2}}) \Delta \eta \Delta \zeta \\ + [(G_{j+\frac{1}{2}} - G_{j-\frac{1}{2}}) - (G_{j+\frac{1}{2}}^v - G_{j-\frac{1}{2}}^v)] \Delta \xi \Delta \zeta \\ + [(H_{k+\frac{1}{2}} - H_{k-\frac{1}{2}}) - (H_{k+\frac{1}{2}}^v - H_{k-\frac{1}{2}}^v)] \Delta \xi \Delta \eta = \Delta \xi \Delta \eta \Delta \zeta S \end{aligned} \quad (3.1)$$

Defining the central difference operator  $\delta$  as  $\delta_l ( ) = ( )_{l+\frac{1}{2}} - ( )_{l-\frac{1}{2}}$  and noting that the finite volume cell has sides of unit length, equation (3.1) can be rewritten as:

$$\frac{\partial Q}{\partial \tau} + \delta_i(F) + \delta_j(G - G^v) + \delta_k(H - H^v) = S \quad (3.2)$$

In the above definition of  $\delta$ ,  $l + \frac{1}{2}$  represents the face adjacent to the cell center in the positive direction of  $l$  and  $l - \frac{1}{2}$  represents the face adjacent to the cell center in the negative direction of  $l$ , where  $l = i, j, k$  for  $\xi, \eta, \zeta$  directions respectively.

### 3.2 Implicit Formulation

An implicit scheme is utilized to numerically integrate equation (3.2) because these schemes can handle large CFL numbers. In problems involving viscous computations, very fine grid spacing is chosen to resolve the viscous effects, due to which the tolerable minimum time step cannot be too small for the code

to have any practical value [2]. A first-order time-accurate implicit scheme to numerically solve equation (3.2) can be implemented by the following algebraic equation:

$$\Delta Q^n = - \Delta \tau (R^{n+1}) \quad (3.3)$$

where

$$\begin{aligned} \Delta Q^n &= Q^{n+1} - Q^n \\ R^{n+1} &= \delta_i (F)^{n+1} + \delta_j (G)^{n+1} + \delta_k (H)^{n+1} - \\ &\quad \delta_j (G^v)^{n+1} - \delta_k (H^v)^{n+1} - S^{n+1} \end{aligned} \quad (3.4)$$

As can be observed from the above equation, the convective and diffusive fluxes and the source term are all treated implicitly.

### 3.3 Newton's Formulation

The Newton's iteration method is used in this work to solve equation (3.4). A detailed explanation of the method is presented in [2] and [7]. For a system of nonlinear equations the Newton's method can be stated as [7]:

$$F'(x^k) (x^{k+1} - x^k) = - F(x^k) \quad (3.5)$$

Dividing equation (3.3) by  $J$ , will result in

$$\Delta q^n = - \overline{\Delta \tau} (R^{n+1}) \quad (3.6)$$

where

$$\overline{\Delta \tau} = \frac{\Delta \tau}{J} \quad (3.7)$$

The Newton's method can now be applied to the following vector equation:

$$L(q^{n+1}) = 0 \quad (3.8)$$

where

$$L(q^{n+1}) = q^{n+1} - q^n + \overline{\Delta\tau} (R^{n+1}) \quad (3.9)$$

The resulting matrix equation is:

$$\begin{aligned} [ I - \overline{\Delta\tau} \left( \frac{\partial S}{\partial q} \right)^{*,k-1} + \overline{\Delta\tau} (M)^{*,k-1} \cdot ] \Delta q^{k-1} = \\ - [ q^{k-1} - q^n + \overline{\Delta\tau} (R^{*,k-1}) ] \end{aligned} \quad (3.10)$$

The operator  $\cdot$  indicates that the difference operator  $M$  acts on the delta form of the unknown vector  $\Delta q^{k-1}$ , where  $\Delta q^{k-1} = q^k - q^{k-1}$  [2]. It can be observed from equation (3.10), that the time derivative term is present in the residual which arises by applying the Newton's method to the nonlinear system of equations. The sub-iterations help in obtaining a better approximation of the solution at each time step. This method, is therefore, better for unsteady problems. The various operators and terms appearing in equation (3.10) are defined as follows:

$$\begin{aligned} M^{*,k-1} \cdot &= \delta_i (A)^{*,k-1} \cdot + \delta_j (B)^{*,k-1} \cdot + \delta_k (C)^{*,k-1} \cdot - \\ &\delta_j (B^v)^{*,k-1} \cdot - \delta_k (C^v)^{*,k-1} \cdot \\ \text{where } A &= \frac{\partial F}{\partial q}, \quad B = \frac{\partial G}{\partial q}, \quad C = \frac{\partial H}{\partial q}, \quad B^v = \frac{\partial G^v}{\partial q}, \quad C^v = \frac{\partial H^v}{\partial q} \quad (3.11) \\ R^{*,k-1} &= \delta_i (F)^{*,k-1} + \delta_j (G)^{*,k-1} + \delta_k (H)^{*,k-1} - \\ &\delta_j (G^v)^{*,k-1} - \delta_k (H^v)^{*,k-1} - S^{*,k-1} \end{aligned}$$

The superscript  $*$  is used in the above equation to specify the time level for computing the metric terms. Janus [13] found that in order to maintain the mass flow without discontinuities when crossing the interface between a rotor and a stator, the metric terms at old time level  $n$  and  $q^0$  should be used for the first iteration. For the subsequent iterations, the metric terms at the present

level  $n + 1$  and  $q^{k-1}$  are used.  $A$ ,  $B$ , and  $C$  are the flux Jacobians, which are  $5 \times 5$  matrices with real eigenvalues. The form of the flux vectors derived in chapter 2 is identical to the flux vectors obtained in the absolute frame formulation. The derivation of the transformed flux Jacobians and their eigensystem is given in detail in Janus's thesis [8].

### 3.3.1 Flux Vector Splitting

The flux Jacobians have real eigenvalues which correspond to wave propagating speeds in each curvilinear direction. The sign of the eigenvalues dictates what information should be used for the evaluation of the fluxes. To incorporate this approach the flux vectors are split using the Steger-Warming flux vector splitting method described in [9]. The flux vectors are split as follows:

$$\begin{aligned} F &= F^+ + F^- \\ G &= G^+ + G^- \\ H &= H^+ + H^- \end{aligned} \tag{3.12}$$

where the superscript of plus denotes the flux sub-vector corresponding to the positive eigenvalue so that this flux sub-vector is computed using information from the negative direction. Similarly, the flux sub-vector with the superscript of minus is evaluated using information from the positive direction. Utilizing this concept a new set of flux Jacobians can be formulated as follows:

$$\begin{aligned} A^+ &= \frac{\partial F^+}{\partial q}, & B^+ &= \frac{\partial G^+}{\partial q}, & C^+ &= \frac{\partial H^+}{\partial q} \\ A^- &= \frac{\partial F^-}{\partial q}, & B^- &= \frac{\partial G^-}{\partial q}, & C^- &= \frac{\partial H^-}{\partial q} \end{aligned} \tag{3.13}$$

The detailed derivation of these new flux Jacobians is available in Belk's dissertation [10].

### 3.3.2 Viscous Flux Jacobian

The viscous flux Jacobians  $B^v$  and  $C^v$ , defined in equation (3.11) are computed numerically in this study. The numerical derivative used to obtain the elements of the Jacobian matrix is [11]:

$$a_{lm} = \frac{F_l(x + he_m) - F_l}{h} \quad (3.14)$$

where  $e_m$  is the  $m^{\text{th}}$  unit vector and  $h \approx \sqrt{\text{machine } \varepsilon}$ . As will be explained later in this chapter, the viscous fluxes at a face are functions of the right and left dependent variable vector. Thus, the viscous numerical derivative will consist of two parts which can be written separately as:

$$\begin{aligned} (B_{lm}^v)^+ &= \frac{G_l^v(q_j + he_m, q_{j+1}) - G_l^v(q_j, q_{j+1})}{h} \\ (B_{lm}^v)^- &= \frac{G_l^v(q_j, q_{j+1} + he_m) - G_l^v(q_j, q_{j+1})}{h} \\ (C_{lm}^v)^+ &= \frac{H_l^v(q_k + he_m, q_{k+1}) - H_l^v(q_k, q_{k+1})}{h} \\ (C_{lm}^v)^- &= \frac{H_l^v(q_k, q_{k+1} + he_m) - H_l^v(q_k, q_{k+1})}{h} \end{aligned} \quad (3.15)$$

Equation (3.10) can be reformulated by using the new flux Jacobians as:

$$\begin{aligned} [ I - \overline{\Delta\tau} \left( \frac{\partial S}{\partial q} \right)^{*,k-1} + \overline{\Delta\tau} \{ (M^+)^{*,k-1} \cdot + (M^-)^{*,k-1} \cdot \} ] \Delta q^{k-1} = \\ - [ q^{k-1} - q^n + \overline{\Delta\tau} (R^{*,k-1}) ] \end{aligned} \quad (3.16)$$

where

$$\begin{aligned}
(M^+)^{*,k-1} &= \delta_i (A^+)^{*,k-1} + \delta_j (B^+)^{*,k-1} + \delta_k (C^+)^{*,k-1} \\
&\quad - \delta_j [(B^v)^+]^{*,k-1} - \delta_k [(C^v)^+]^{*,k-1} \\
(M^-)^{*,k-1} &= \delta_i (A^-)^{*,k-1} + \delta_j (B^-)^{*,k-1} + \delta_k (C^-)^{*,k-1} \\
&\quad - \delta_j [(B^v)^-]^{*,k-1} - \delta_k [(C^v)^-]^{*,k-1}
\end{aligned} \tag{3.17}$$

The difference expressions that have been mentioned till now are first order accurate in time. A general form of equation (3.16) which incorporates a wide variety of different time accurate schemes is written below [2]:

$$\begin{aligned}
\left[ \frac{1 + \psi}{\theta \Delta \tau} I - \left( \frac{\partial S}{\partial q} \right)^{*,k-1} + (M^+ \cdot + M^- \cdot)^{*,k-1} \right] \Delta q^{k-1} = \\
- \frac{1 + \psi}{\theta \Delta \tau} \left[ q^{k-1} - q^n - \frac{1}{1 + \psi} \left\{ \Delta \tau [ (\theta - 1) R^{n,n} - \theta R^{*,k-1} ] \right. \right. \\
\left. \left. + \psi \Delta q^{n-1} \right\} \right]
\end{aligned} \tag{3.18}$$

A few important time accurate schemes are Euler implicit ( $\theta = 1$ ,  $\psi = 0$ ), three-point backward ( $\theta = 1$ ,  $\psi = 1/2$ ), and trapezoidal ( $\theta = 1/2$ ,  $\psi = 0$ ). The first scheme is first order accurate whereas the other two are second order accurate in time. The three point backward scheme has been used for the work carried out in this study.

### 3.4 Flux Formulation

The computation of the RHS of equation (3.18) requires a method for the computation of the fluxes. The term  $R$  defined in equation (3.4), consists of convective and diffusive flux terms, each of which is computed differently.

#### 3.4.1 Convective Flux Computation

The convective fluxes are hyperbolic in nature which implies that the ei-

genvalues associated with the flux Jacobians are real. Thus, there is a preferred direction of information propagation in such systems. Thus, to be consistent with the physics of the problem one needs to use the method of upwinding to evaluate the convective fluxes. One such method is Roe's flux formulation which is a flux difference split scheme [12]. The method entails solving an approximate Riemann problem exactly at each cell face. However, Roe's method is first order accurate in space which is too dissipative for simulation of realistic problems. Higher order accuracy is obtained by adding corrective flux terms with limiters [2]. The limiters act as a switching mechanism to control the addition of the corrective flux terms such that the formulation is higher order in smooth regions. In regions containing shocks or contact discontinuities the formulation is first order accurate because in such regions higher order schemes are dispersive. The limiters used in the corrective flux terms are Roe's Superebee, van Leer's and minmod limiters. The detailed development of the above formulation is presented in [13], [14], and [15].

### 3.4.2 Diffusive Flux Computation

The evaluation of the diffusive fluxes defined in (2.45) requires the numerical representation of derivatives needed for the stress calculations which can be noted in equations (2.47) and (2.48). The metric terms such as  $\xi_x$ ,  $\xi_y$ , ..., are also needed instead of  $J\xi_x$ ,  $J\xi_y$ , ..., which are the projections of the face areas in the Cartesian directions and are computed in the code. The diffusive fluxes are parabolic in nature so that there is no preferred direction of information propagation for systems. Thus, the central differencing scheme is the most popular and easiest way to compute the derivatives appearing in the diffusive



fluxes [2]. The implementation of the above approach is illustrated by considering an example stress term,  $\tau_{xx}$ :

$$\tau_{xx} = \frac{1}{\text{Re}} \frac{2}{3} \mu \left[ 2k_x \frac{\partial u}{\partial k} - k_y \frac{\partial v}{\partial k} - k_z \frac{\partial w}{\partial k} \right]$$

The following numerical formulae are used to calculate the various terms that appear in the above equation:

$$\left( k_x \right)_{k+\frac{1}{2}} = \frac{\left( Jk_x \right)_{k+\frac{1}{2}}}{\frac{1}{2} \left( J_k + J_{k+1} \right)}, \quad \left( k_y \right)_{k+\frac{1}{2}} = \frac{\left( Jk_y \right)_{k+\frac{1}{2}}}{\frac{1}{2} \left( J_k + J_{k+1} \right)}, \dots \quad (3.19)$$

$$\left( \frac{\partial u}{\partial k} \right)_{k+\frac{1}{2}} = u_{k+1} - u_k, \quad \left( \frac{\partial v}{\partial k} \right)_{k+\frac{1}{2}} = v_{k+1} - v_k, \dots \quad (3.20)$$

The central difference scheme in equation (3.20) is of second order accuracy.

### 3.4.3 Turbulence Modeling

Equation (2.42), which is the thin-layer Navier-Stokes equation, becomes Reynolds-averaged thin-layer Navier-Stokes equation which is the time averaged Navier-Stokes equation for turbulent flows, when  $\mu$  is written as:

$$\mu = \mu_l + \mu_t \quad (3.21)$$

Similarly the thermal conductivity is written as:

$$k = k_l + k_t \quad (3.22)$$

or

$$k = \frac{\mu}{\text{Pr}(\gamma - 1)} = \frac{\mu_l}{\text{Pr}_l(\gamma - 1)} + \frac{\mu_t}{\text{Pr}_t(\gamma - 1)} \quad (3.23)$$

where  $\text{Pr}_l = 0.72$  and  $\text{Pr}_t = 0.90$  for air [2].

The Baldwin and Lomax turbulence model [16] is used in this study for the calculation of  $\mu_t$ . A detailed description of the model is given in [2]. This mod-

el is a two-layer algebraic eddy viscosity model in which  $\mu_t$  is evaluated differently for the inner and outer layers. Since there is no clear demarcation between the inner and outer layers,  $\mu_t$  at each cell face is calculated by both methods and then the smaller value is chosen [2].

### 3.5 The N-Pass Scheme

Equation (3.18) can be written in the general form as:

$$(L + D + U) X = b \quad (3.24)$$

where  $L$  is strictly lower block triangular,  $D$  is block diagonal and  $U$  is strictly upper block triangular. The system of equations defined above can be solved using the “N-Pass” algorithm. The “N-Pass” algorithm can be viewed as a relaxation scheme based on the symmetric Gauss-Siedel algorithm [17]:

$$\left. \begin{array}{l} (L + D) X^1 + U X^0 = b \\ L X^1 + (D + U) X^2 = b \\ \vdots \\ (L + D) X^{2N-1} + U X^{2N-2} = b \\ L X^{2N-1} + (D + U) X^{2N} = b \end{array} \right\} \begin{array}{l} 1^{\text{st}} \text{ pass} \\ \\ \\ N^{\text{th}} \text{ pass} \end{array} \quad (3.25)$$

The nature of  $L$ ,  $D$ , and  $U$  can be exploited to reduce the number of matrix vector multiplications needed to be carried out [7]. The modified two-pass scheme can be shown to be equivalent to one pass of the “N-Pass” scheme described above. This has been illustrated by considering a representative one-dimensional stencil in [2]. Since, more than two iterations are needed for the Gauss-Siedel iterative method to yield a converged solution, the “N-Pass” scheme allows the scope for a more accurate and stable solver. This is so, because with each additional

pass one can add two additional Gauss-Siedel iterations, which gives a better solution. In this study, only one pass has been used to obtain the solution. This scheme has also been vectorized using the diagonal plane processing developed in [13] and [10].

### 3.6 Boundary Conditions

The characteristic variable boundary conditions as applied to the non-conservative vector form of the transformed Euler equations with source terms developed in [18] is used in this study. For the viscous computations, at the walls, the adiabatic wall, no-slip boundary condition developed in [14] is applied. The inflow boundary condition that is developed in [2] which specifies the reservoir conditions for internal flows, called the total-condition-preserved boundary condition does not change between the two formulations. This is so because inflow is assumed to be uniform at the grid entrance and only in the x-direction which is normal to the plane of rotation. The only difference in the boundary conditions that is made when one changes from the fixed frame approach to the rotating frame approach arises in the subsonic outflow boundary conditions. The subsonic outflow boundary conditions with source terms are coupled with the simple radial equilibrium equation described in [19]. The simple radial equilibrium accounts for the swirl produced downstream of the blades [2].

#### 3.6.1 Subsonic Outflow

Subsonic outflow condition is illustrated by the figure below.

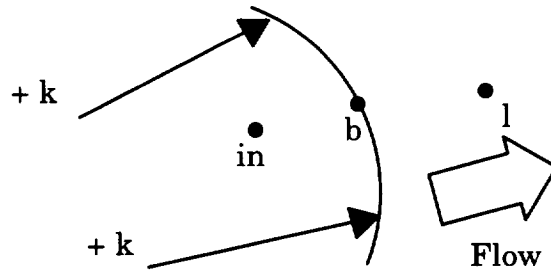


Figure 3.2 Codirectional Outflow

In the above situation, depicted by Figure 3.2 four pieces of information come from inside the computational domain and one from outside. If the outflow boundary is a constant  $\xi$  plane and the outflow is in the positive  $\xi$  direction, then the characteristic variables that are evaluated from inside the computational domain are [18]:

$$\left[ \xi_x \left( \rho - \frac{p}{c_0^2} \right) + \xi_z v - \xi_y w \right]_b = \left[ \xi_x \left( \rho - \frac{p}{c_0^2} \right) + \xi_z v - \xi_y w \right]_{in} + \Gamma_1 \quad (3.26)$$

$$\left[ \xi_y \left( \rho - \frac{p}{c_0^2} \right) - \xi_z u + \xi_x w \right]_b = \left[ \xi_y \left( \rho - \frac{p}{c_0^2} \right) - \xi_z u + \xi_x w \right]_{in} + \Gamma_2 \quad (3.27)$$

$$\left[ \xi_z \left( \rho - \frac{p}{c_0^2} \right) + \xi_y u - \xi_x v \right]_b = \left[ \xi_z \left( \rho - \frac{p}{c_0^2} \right) + \xi_y u - \xi_x v \right]_{in} + \Gamma_3 \quad (3.28)$$

$$\left[ \frac{p |\nabla \xi|}{\varrho_0 c_0} + \xi_x u + \xi_y v + \xi_z w \right]_b = \left[ \frac{p |\nabla \xi|}{\varrho_0 c_0} + \xi_x u + \xi_y v + \xi_z w \right]_{in} + \Gamma_4 \quad (3.29)$$

where  $\Gamma_i = \Delta\tau \frac{|\nabla \xi|}{J} \bar{\Gamma}_i$ ,  $\bar{\Gamma} = P_{\xi,0}^{-1} M^{-1} S$ . The subscript "0" denotes that the matrix  $P_{\xi}^{-1}$  is considered to be locally constant. The  $P_{\xi}^{-1}$  and  $M^{-1}$  are derived in [8] and  $S$  is defined in (2.46) so that one can write the elements of  $\Gamma$  as:

$$\begin{aligned} \Gamma_1 &= \Delta\tau [-\xi_z w \Omega - \xi_y v \Omega] \\ \Gamma_2 &= \Delta\tau [\xi_x v \Omega] \\ \Gamma_3 &= \Delta\tau [\xi_x w \Omega] \\ \Gamma_4 &= \Delta\tau [-\xi_y w \Omega + \xi_z v \Omega] \end{aligned} \quad (3.30)$$

By constructing the grid such that the outflow boundary is normal to the x axis, the metrics  $\xi_y$  and  $\xi_z$  will be zero [19]. Utilizing this result in equations (3.26)-(3.30), the characteristic variables simplify to:

$$\left[ \varrho - \frac{p}{c_0^2} \right]_b = \left[ \varrho - \frac{p}{c_0^2} \right]_{in} \quad (3.31)$$

$$v_b = v_{in} - \Delta\tau w_{av} \Omega \quad (3.32)$$

$$w_b = w_{in} + \Delta\tau v_{av} \Omega \quad (3.33)$$

$$\left( \frac{p}{\varrho_0 c_0} + u \right)_b = \left( \frac{p}{\varrho_0 c_0} + u \right)_{in} \quad (3.34)$$

where  $\varrho_0$  and  $c_0$  are reference quantities.  $v_{av}$  and  $w_{av}$  are calculated using phantom points which are explained later in this section. The calculation of

pressure at the outflow boundary is carried out by using the result from the first three equations above in the radial equilibrium equation [19]:

$$\frac{\partial p}{\partial r} = \left[ \frac{\rho}{r} v_{\theta}^2 \right]_b \quad (3.35)$$

A first order finite difference scheme is used to evaluate the derivative and the right hand side is calculated as the average of the quantity at the two points being considered. This procedure will yield the following algebraic equation:

$$\frac{p_2 - p_1}{r_2 - r_1} = \frac{1}{2} \left[ \frac{\left( \frac{p_1}{c_{01}^2} + a_1 \right) v_{\theta 1}^2}{r_1} + \frac{\left( \frac{p_2}{c_{02}^2} + a_2 \right) v_{\theta 2}^2}{r_2} \right] \quad (3.36)$$

where  $a = \left[ \rho - \frac{p}{c_0^2} \right]_{in}$  and the subscripts 1 and 2 denote the points along the

spanwise direction. Letting  $f = \frac{v_{\theta}^2}{c_0^2 r}$  and  $g = \frac{a v_{\theta}^2}{r}$  one gets the following ex-

pression:

$$p_2 = \frac{p_1 + \frac{(r_2 - r_1)}{2} (p_1 f_1 + g_1 + g_2)}{1 - \frac{(r_2 - r_1)}{2} f_2} \quad (3.37)$$

The calculation proceeds from the casing (maximum value of  $r$ ), where the pressure is taken to be the specified back pressure, to the hub. Once the pressure at the boundary is determined, the density and  $u$  can be calculated from the equations (3.31) and (3.34) respectively.

To implement the boundary conditions a layer of phantom points just outside the computational domain is used. The conditions at these points are deter-

mined by the following relations:

$$\psi_p = 2\psi_b - \psi_{in} \quad (3.38)$$

where  $\psi$  is any of the primitive variables and subscript  $p$  denotes a phantom point. Once the primitive variables are determined, the conservative variables can be calculated at the phantom points. Using the above definition,  $v_{av}$  and  $w_{av}$  appearing in equations (3.32) and (3.33) can be written as:

$$\begin{aligned} v_{av} &= \frac{v_{in} + v_p}{2} \\ w_{av} &= \frac{w_{in} + w_p}{2} \end{aligned} \quad (3.39)$$

It should be noted that  $v_p$  and  $w_p$  in equation (3.39) are calculated using the solution at the previous time step.

## CHAPTER IV

### RESULTS

The aim of the work carried out in this study is to show that, for turbomachinery applications, solving the Navier-Stokes equation cast in the rotating frame has a significant advantage over solving the same in fixed coordinates. However, one has to be sure that the change in formulation does not introduce any additional inaccuracy which will degrade the solution. The test case chosen in this study to validate the formulation is NASA's Rotor 67, which has one row of rotating blades.

All the computations were performed on the SGI Challenge 10000 XL computer. The calculations have been carried out with third order spatial and second order temporal accuracy. The higher order computations and viscous computations are delayed for a few cycles.

#### 4.1 Rotor 67

The first stage rotor of a NASA Lewis designed two-stage fan, Rotor 67, has been used to validate the code for a single-rotating geometry in internal flow. The test case is a low-aspect-ratio, damperless, transonic axial-flow fan rotor. It has 22 blades of multiple-circular-arc design and no inlet guide vanes. The inlet relative Mach number at the rotor tip was 1.38 at the designed tip speed of 428.9 m/sec (16,043 rpm). The designed pressure ratio for the rotor is 1.63 at a mass flow rate of 33.25 Kg/sec [2].



The grid used for the computations is very coarse. An H-type grid for the whole computational domain was generated by TIGER, an interactive turbomachinery grid generation code developed by Shih [20]. The grid has dimensions of 55x31x25 with twenty one points on the blade axially and twenty six points in the spanwise direction. There is a gap clearance between the blade tip and the casing. Since this case is at zero angle of attack, only one blade passage needs to be simulated by taking advantage of the symmetry.

Total-condition-preserved B.C. is used to apply constant uniform conditions at the upstream boundary. Axisymmetric B.C.s are used for re-entry boundaries. No-slip B.C.s are used on the blades, hub and casing. At the exit plane, the radial equilibrium boundary conditions with the source terms are applied with the back pressure specified at the radial location corresponding to the casing. The Reynolds number based on the tip diameter at the designed speed and standard day conditions was about 8,000,000.

The solution is considered converged when the following are true:

1. The inlet mass flow rate changed less than 0.2% of the average of the maximum and minimum values in 1000 cycles.
2. Mass flow ratio (outlet / inlet) varied between  $1 \pm 0.005$  in 1000 cycles.

For the above test case three conditions were run with the non-dimensional back pressures of 0.75, 0.85, and 0.90 which correspond to choke, near peak efficiency and near stall conditions respectively. Since the problem can be viewed as a steady state flow in the rotating frame, the relative frame code is run with both, local time stepping and minimum time stepping. The absolute frame code can only be run with minimum time stepping. Figures 4.1, 4.3, and 4.5 show

a comparison of mass flow histories between the relative frame and the absolute frame codes, for the three conditions, respectively. The comparison of the behavior of the mass flow ratio is presented in Figures 4.7, 4.9, and 4.11.

As can be observed from the mass flow histories, the absolute frame code requires a much longer time to yield a satisfactorily converged solution. The absolute code was run with a CFL=70 which corresponds to 2600 time steps per revolution, and with 2 Newton sub-iterations per time step. When using local time stepping the rotating frame code was run with a CFL=50; no Newton sub-iterations. While using minimum time stepping the relative code was run with a CFL=10000, corresponding to 18 time steps per revolution. However, the initial 400 cycles were run with a CFL=500. Thereafter, the CFL was increased to 10000.

The absolute code requires 10400 cycles (4 revolutions) to produce a converged solution, whereas the rotating frame code requires a minimum of 1500 cycles to give a converged solution when run using minimum time stepping. When local time stepping was used, a minimum of 1500 cycles were needed. Thus, there is no significant advantage of using the local time stepping method with the rotating frame code. This can be attributed to the very high CFL that can be used when running with the minimum time stepping method. It can be observed from the plots that as the back pressure is increased progressively, more number of cycles are required to obtain a converged solution. The final inlet mass flow rates between the two formulations varies by less than  $\pm 1\%$ . The advantage can be better appreciated on a semi-log plot which has been shown in Figures 4.2, 4.4, and 4.6 for inlet mass flow and Figures 4.8, 4.10, and 4.12

for mass flow ratio. Another observation that can be made from the plots is that the mass flow ratio settles down much faster than the inlet mass flow for all the three cases.

The speedup that one observes due to the above description is huge. The absolute frame code requires 38 hours of running time to complete one revolution, whereas the relative frame code requires 10 hours running time for 2000 cycles on an SGI Challenge 10000 XL. The CPU times required by the two formulations for the three different conditions are illustrated in the table below. Since there was no difference in the number of cycles required with the relative frame formulation when using local time stepping or minimum time stepping, the CPU times corresponding to the relative method using both approaches is the same.

Table 4.1

Performance Enhancement

METHOD	TIME (hrs.) back pr. = 0.75	TIME (hrs.) back pr. = 0.85	TIME (hrs.) back pr. = 0.90
RELATIVE	7.5	12.5	15
ABSOLUTE	152	171	190

In order to ensure the accuracy of the solution, a comparison is made between the relative Mach number contours obtained from by solving the two for-

mulations. The comparisons are made at two operating points, one near peak efficiency and the other near stall condition, and at 10%, 30%, and 70% span locations from the blade tip. The operating point near peak efficiency occurs at a non-dimensional back pressure of 0.85 which results in an inlet mass flow of 33.89 kg/sec, which is 97.86% of the computed choked flow, which occurs at a non-dimensional back pressure of 0.75. For the same back pressure the absolute frame code has a mass flow rate which is 98.39% of the choked flow rate. Figures 4.13-4.15 illustrate the comparisons for this operating point and for 10%, 30%, and 70% spanwise locations respectively.

The near stall condition occurs at a non-dimensional pressure of 0.90. The relative frame code yields an inlet mass flow rate of 32.49 kg/sec which is 93.82% of the computed choked flow rate, for this condition. The absolute frame yields an inlet mass flow rate which is 94.91% of the choked flow rate. The relative Mach number contours for this condition at the various spanwise locations are shown in Figures 4.16-4.18.

It can be observed from the figures that there is a good agreement between the relative Mach number contours. Thus, it can be concluded that the formulation presented in this study does not introduce any additional errors. The discrepancies between the computed relative Mach number contour plots and the experimental plots are the same for the two formulations and are not discussed in this work.

A detailed description of the flow field and the agreement and discrepancies between computed and experimental results is given in [2]. Another observation that was made during the course of this study is that the relative

frame code does produce a converged solution for a non-dimensional back pressure of 0.95 whereas the absolute frame code exhibits a stall condition beyond a non-dimensional back pressure 0.90.

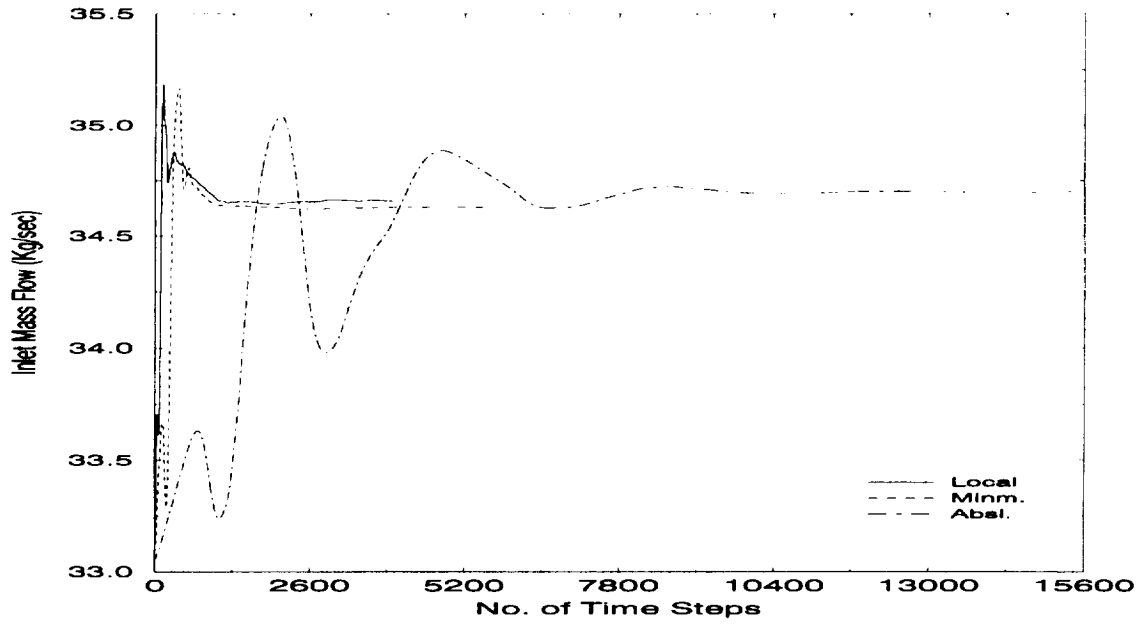


Figure 4.1 Mass Flow History (back pr. = 0.75)

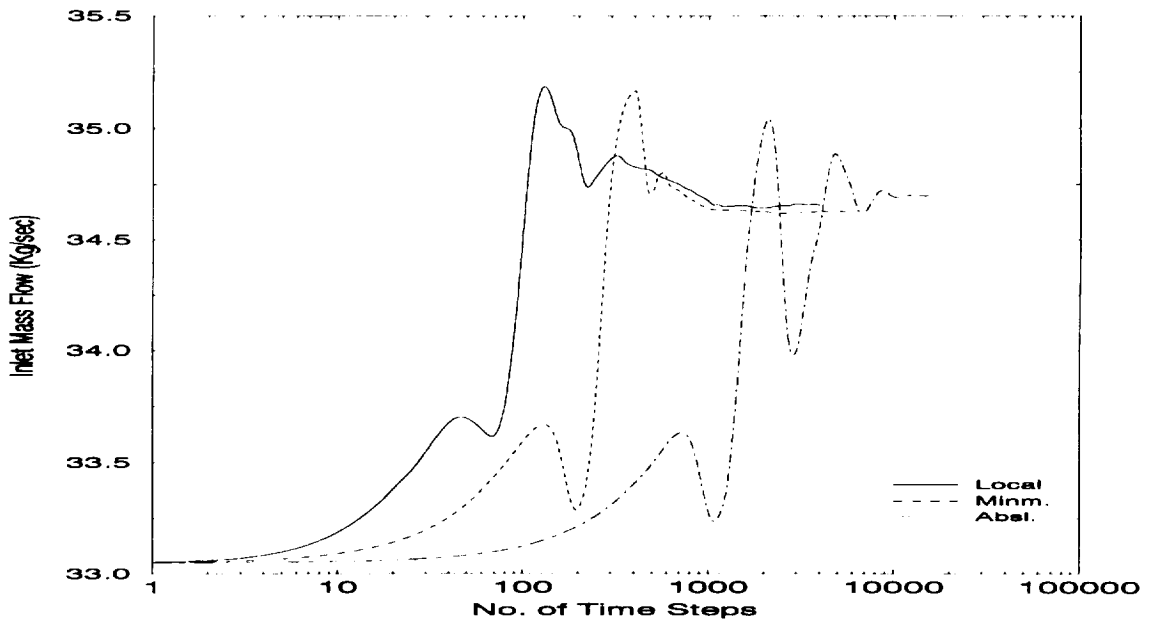


Figure 4.2 Mass Flow History (log-linear, back pr. = 0.75)

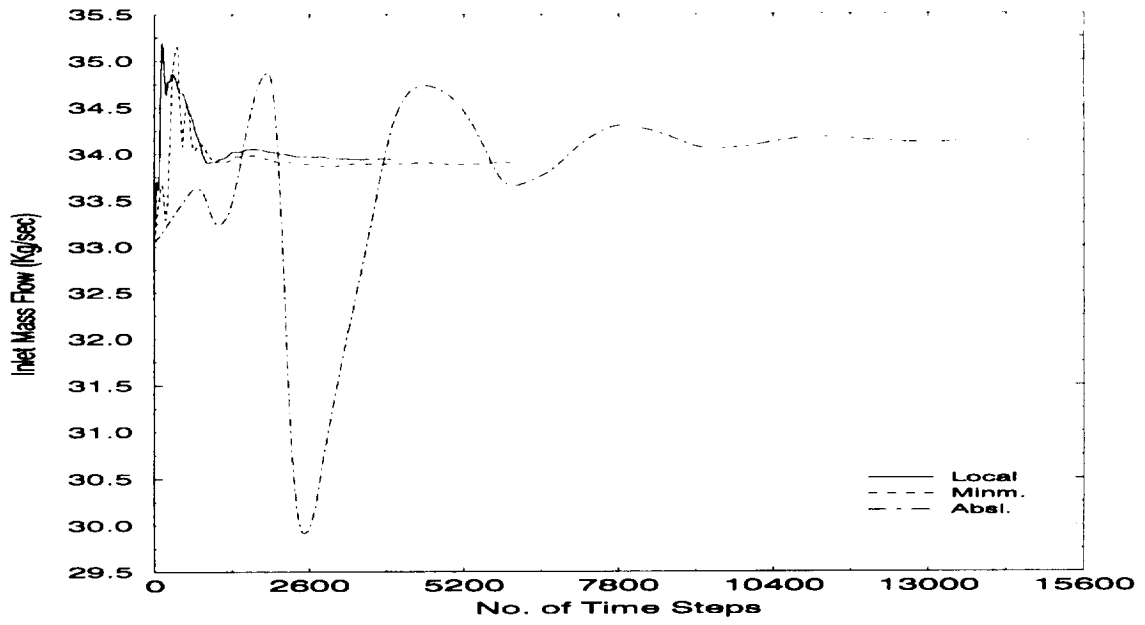


Figure 4.3 Mass Flow History (back pr. = 0.85)

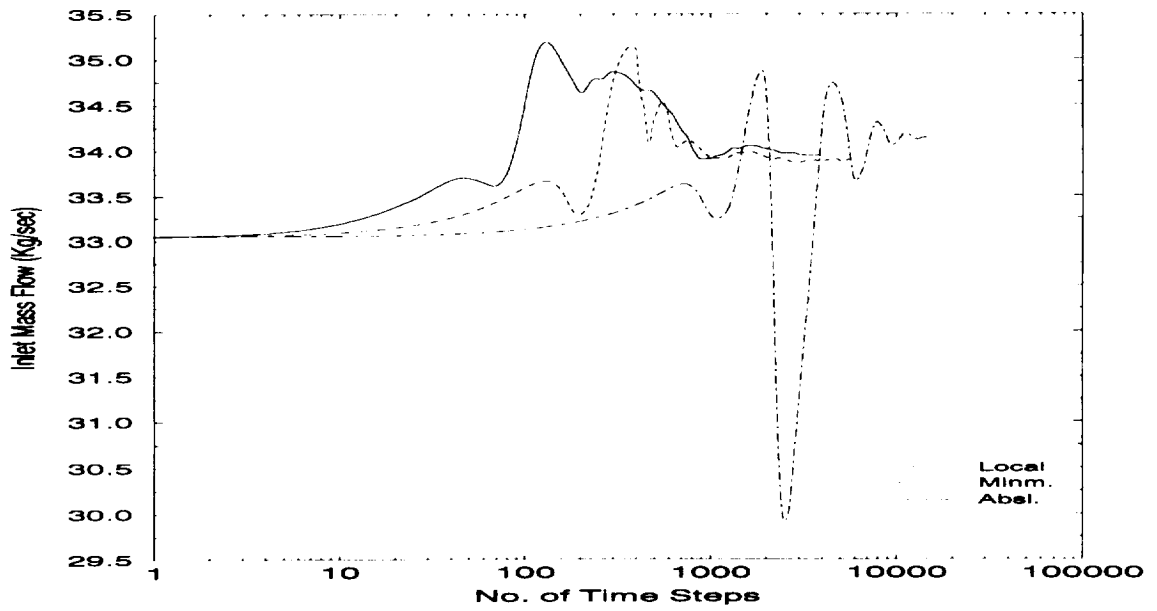


Figure 4.4 Mass Flow History (log-linear, back pr. = 0.85)

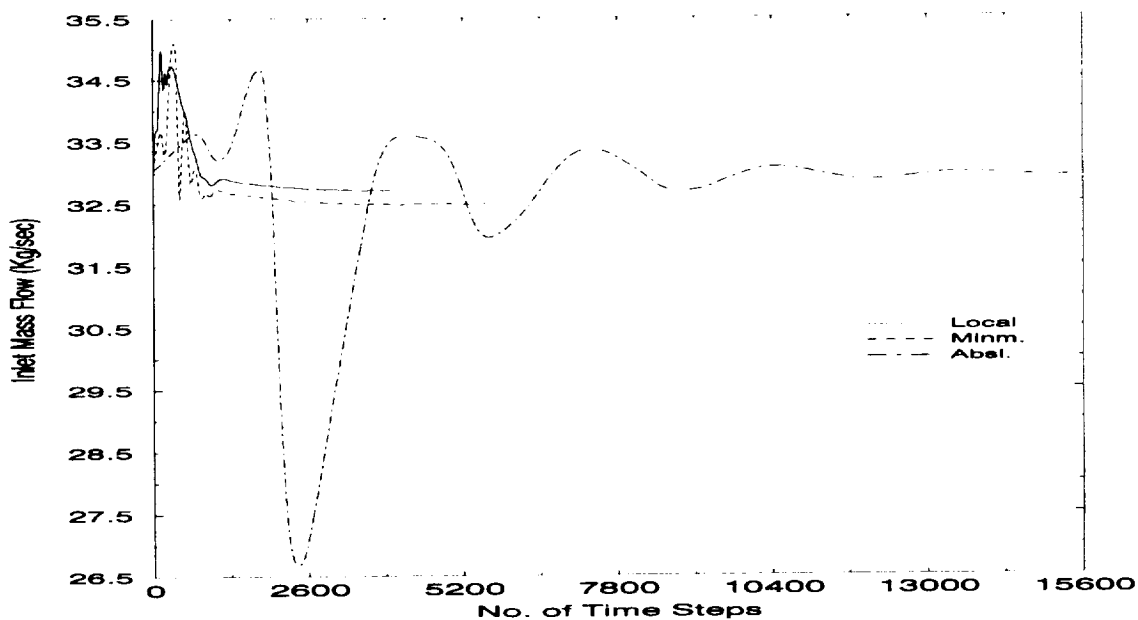


Figure 4.5 Mass Flow History (back pr. = 0.90)

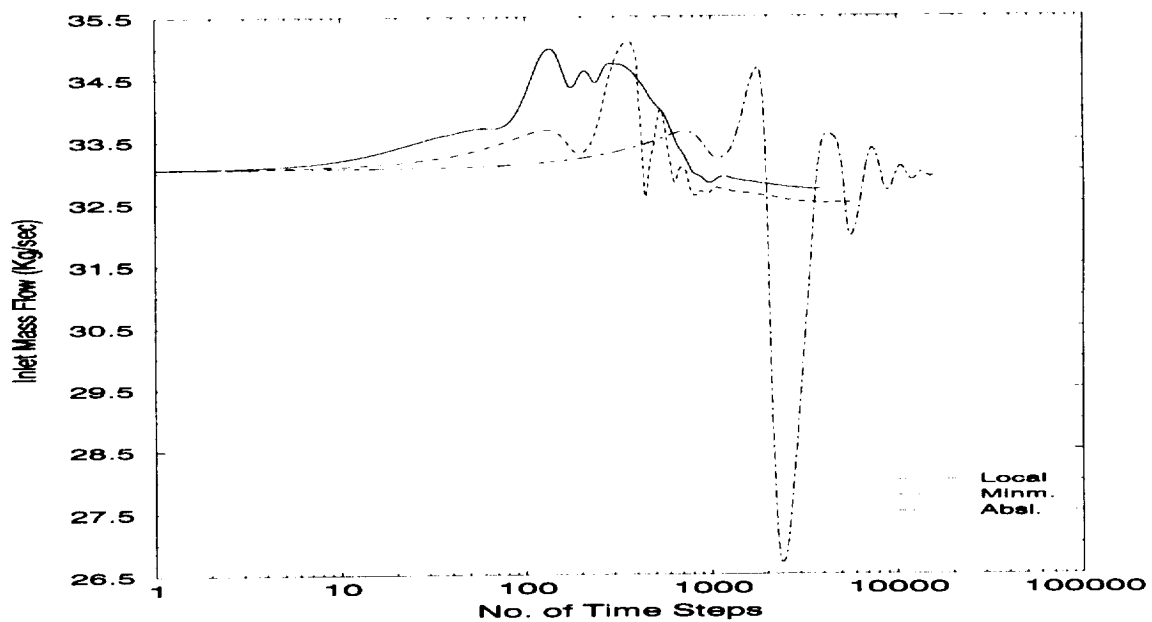


Figure 4.6 Mass Flow History (log-linear, back pr. = 0.90)



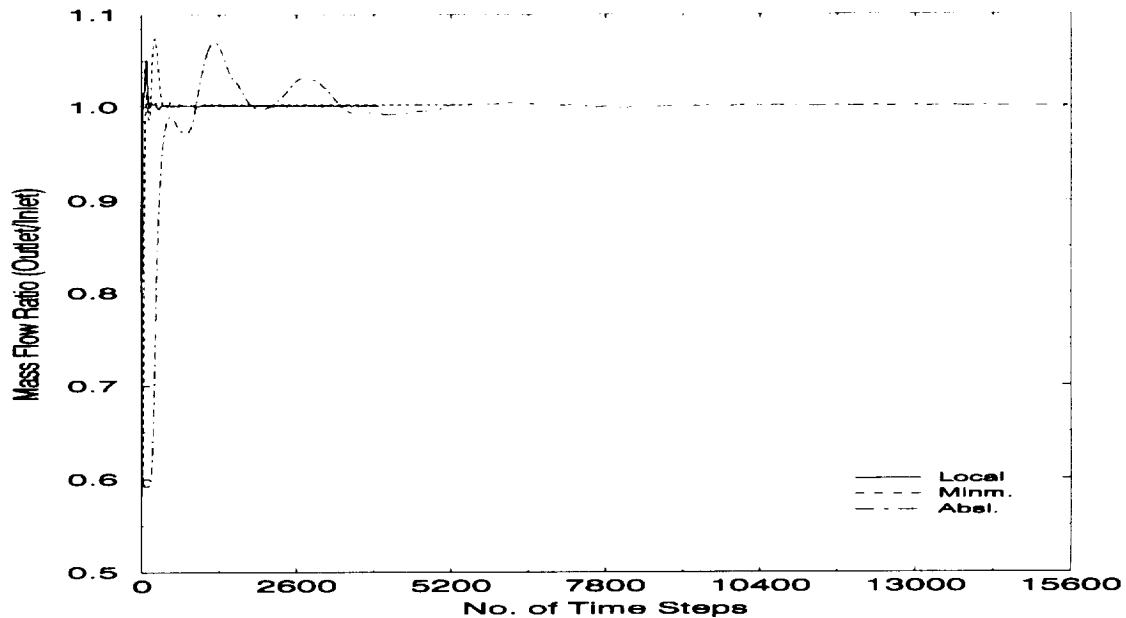


Figure 4.7 Mass Flow Ratio History (back pr. = 0.75)

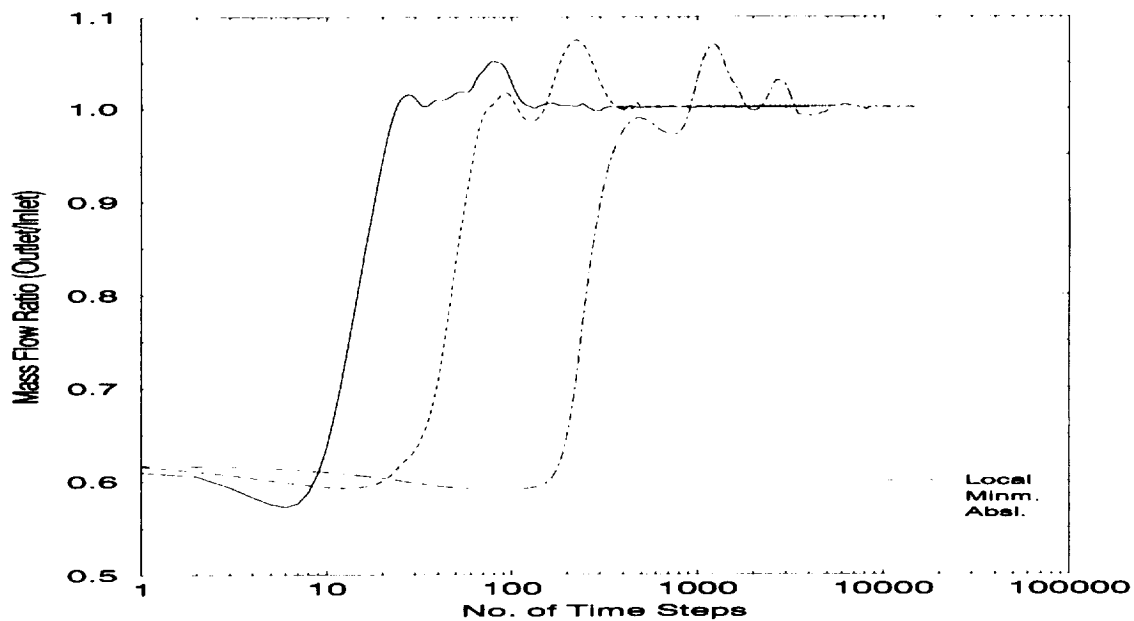


Figure 4.8 Mass Flow Ratio History (log-linear, back pr. = 0.75)

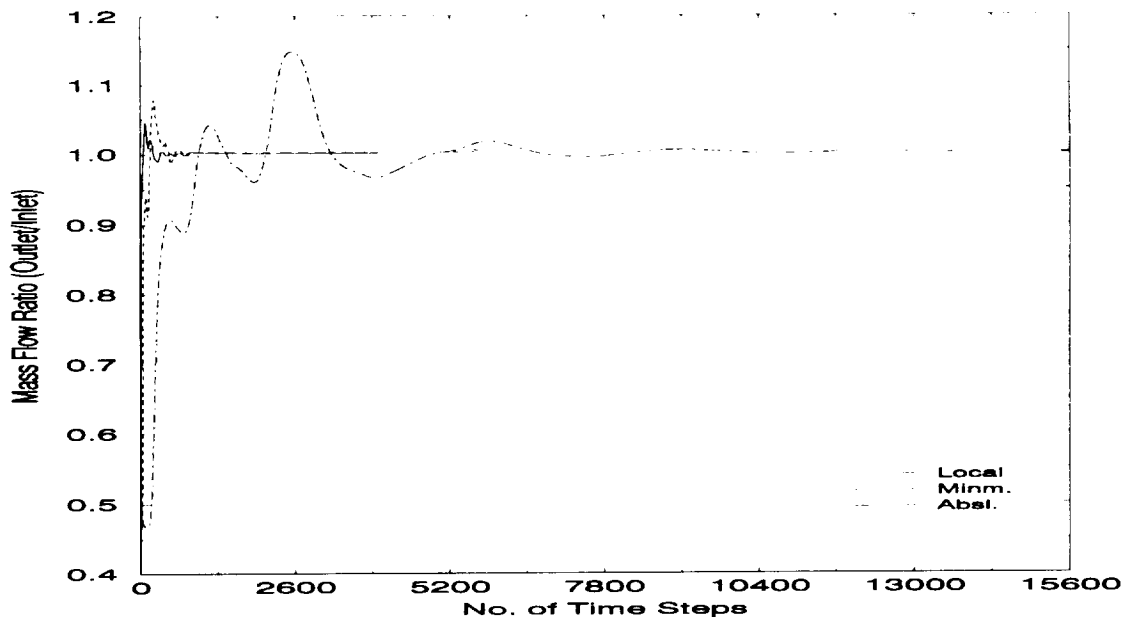


Figure 4.9 Mass Flow Ratio History (back pr. = 0.85)

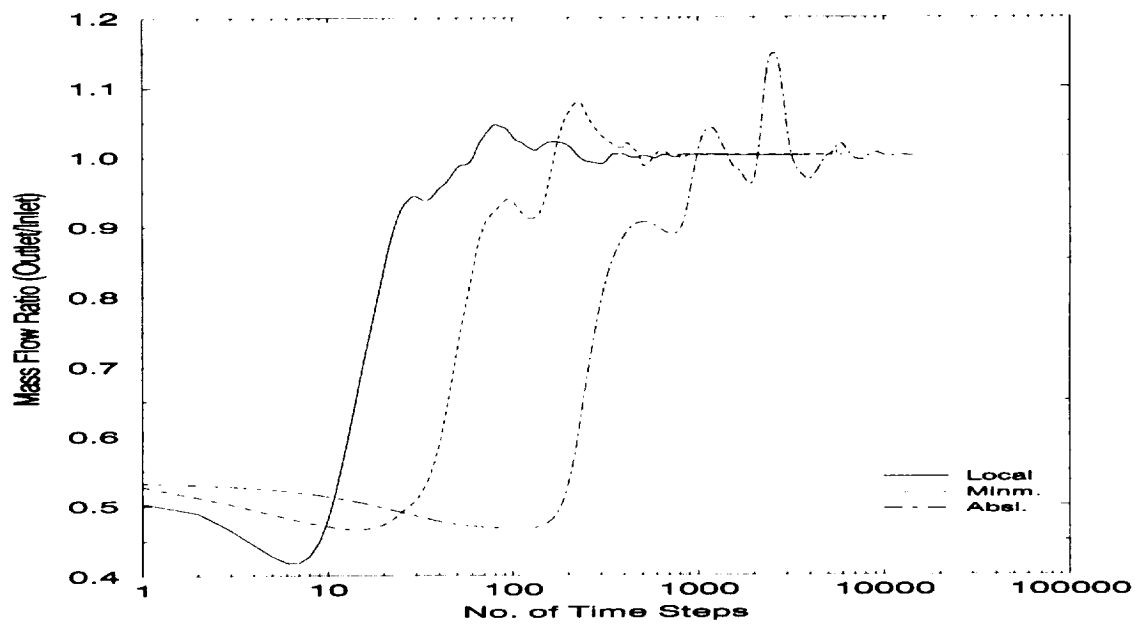


Figure 4.10 Mass Flow Ratio History (log-linear, back pr. = 0.85)

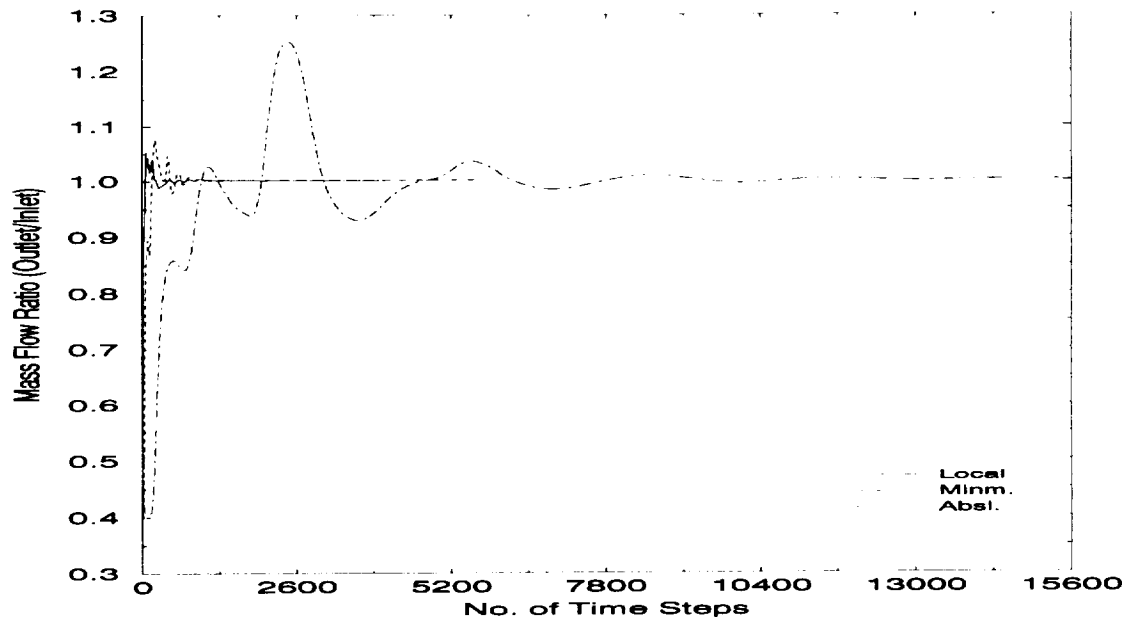


Figure 4.11 Mass Flow Ratio History (back pr. = 0.90)

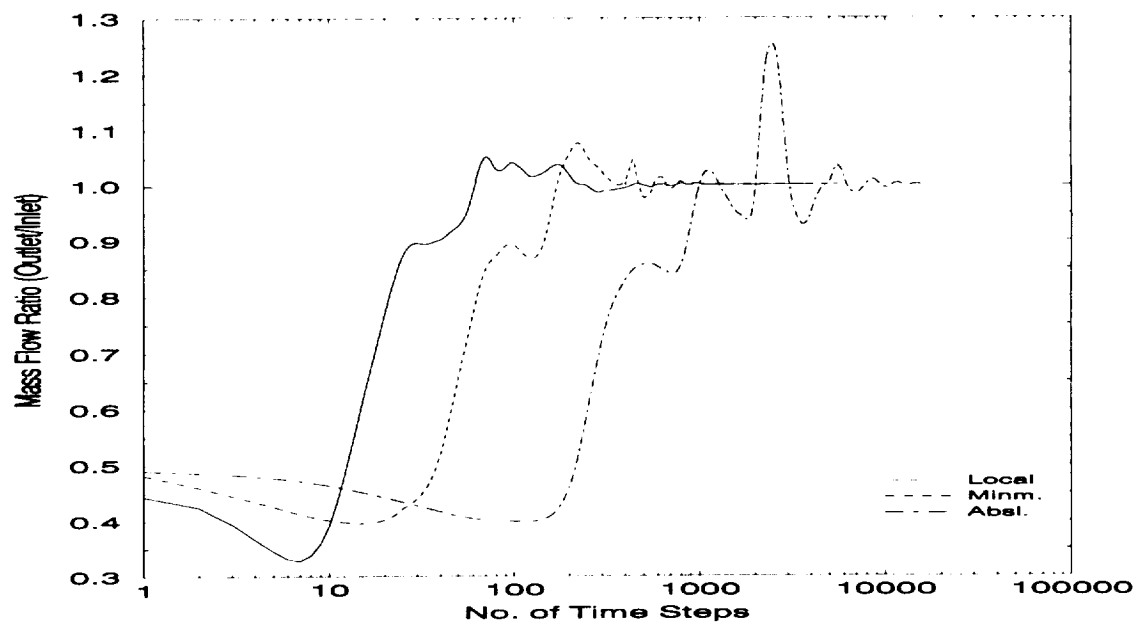


Figure 4.12 Mass Flow Ratio History (log-linear, back pr. = 0.90)

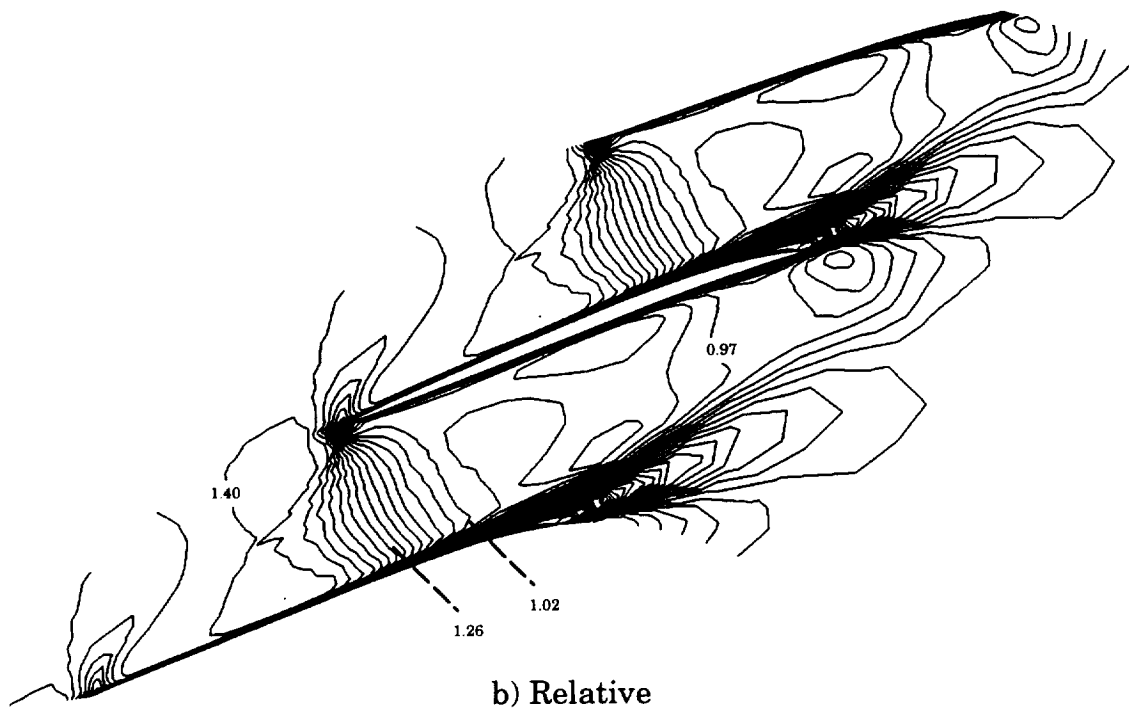
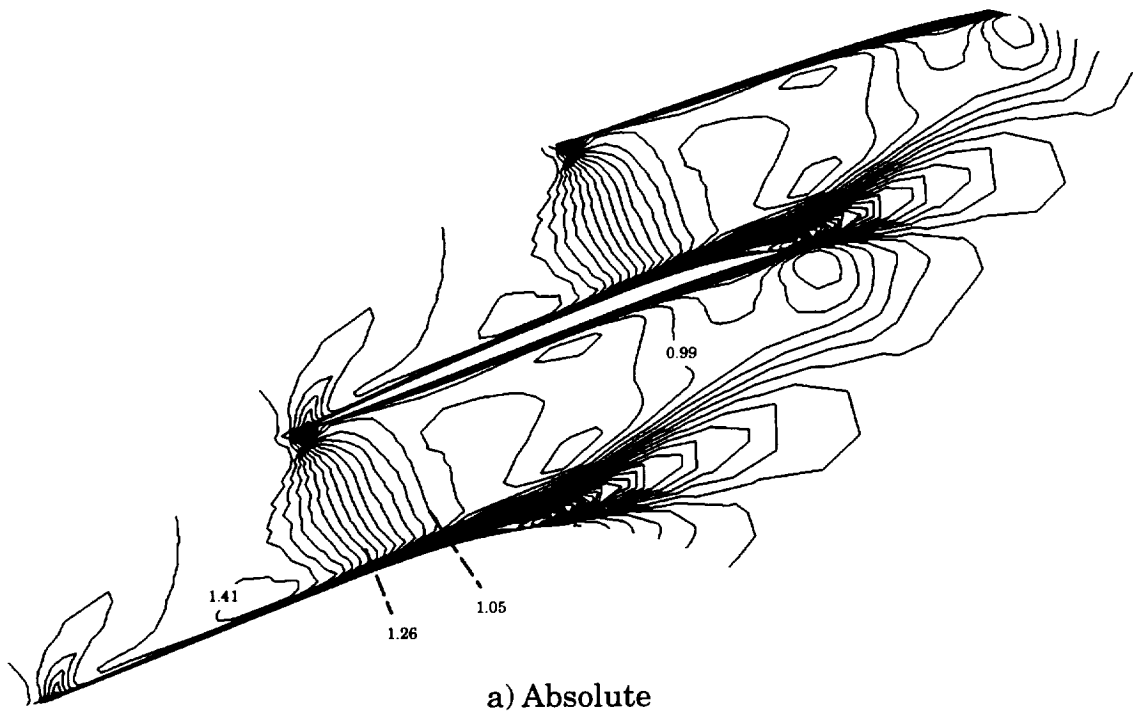


Figure 4.13 Relative Mach No. Contours at 10% Span for Near Peak Efficiency

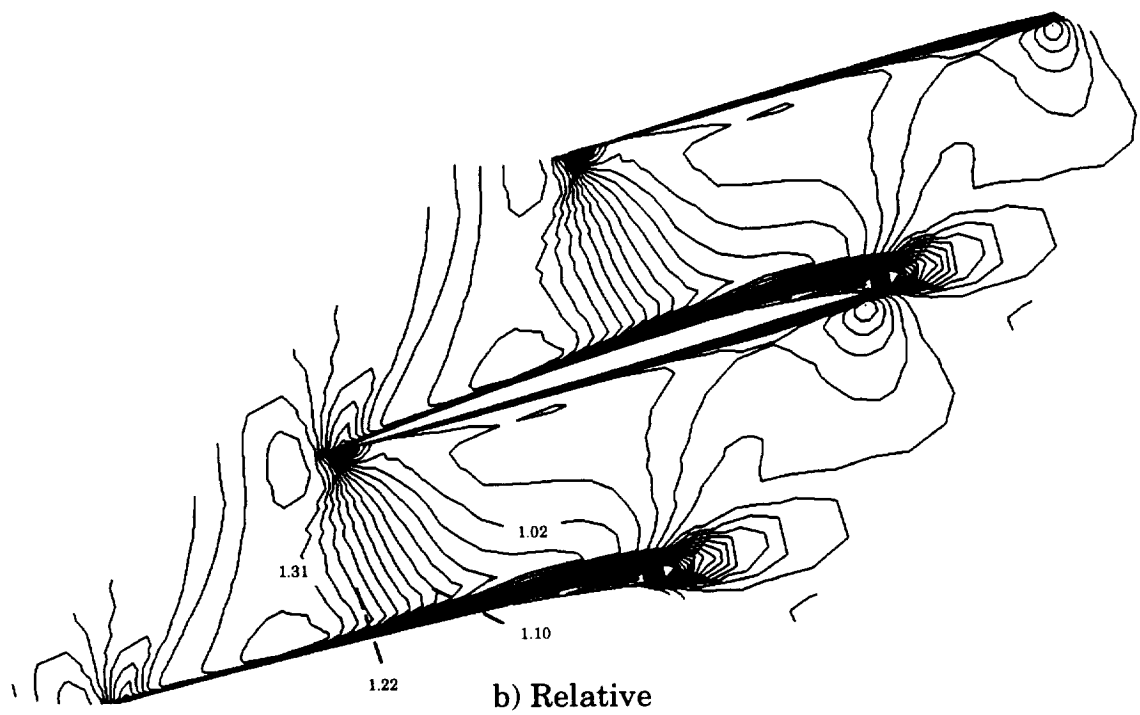
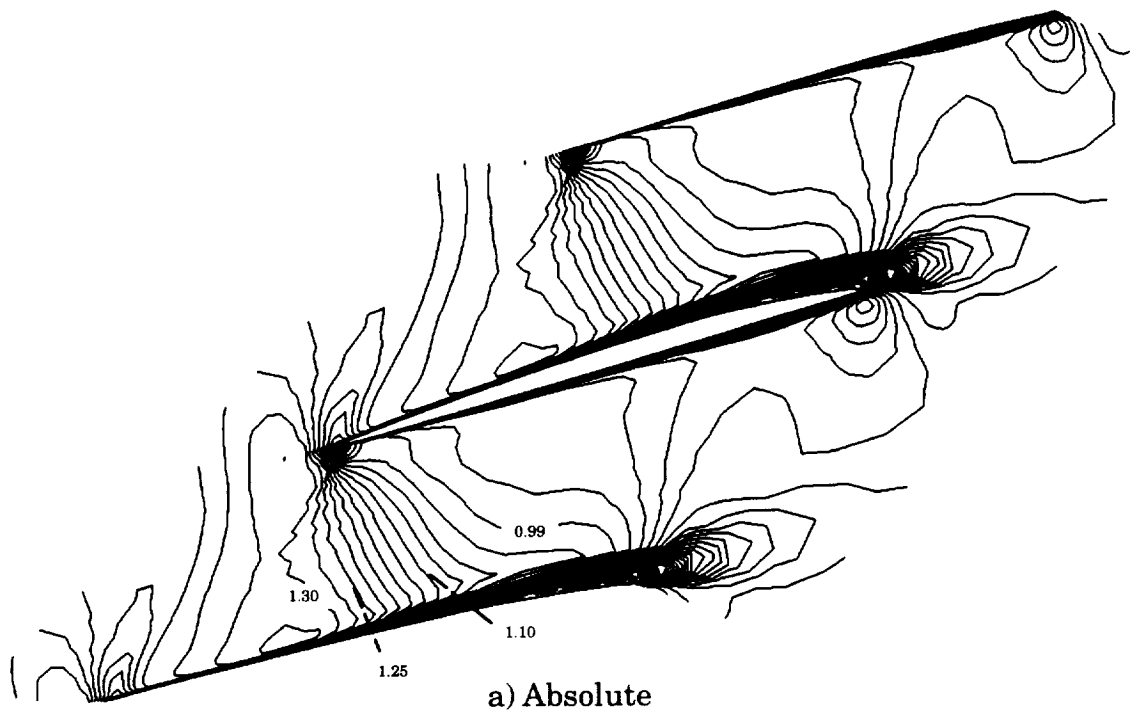


Figure 4.14 Relative Mach No. Contours at 30% Span for Near Peak Efficiency

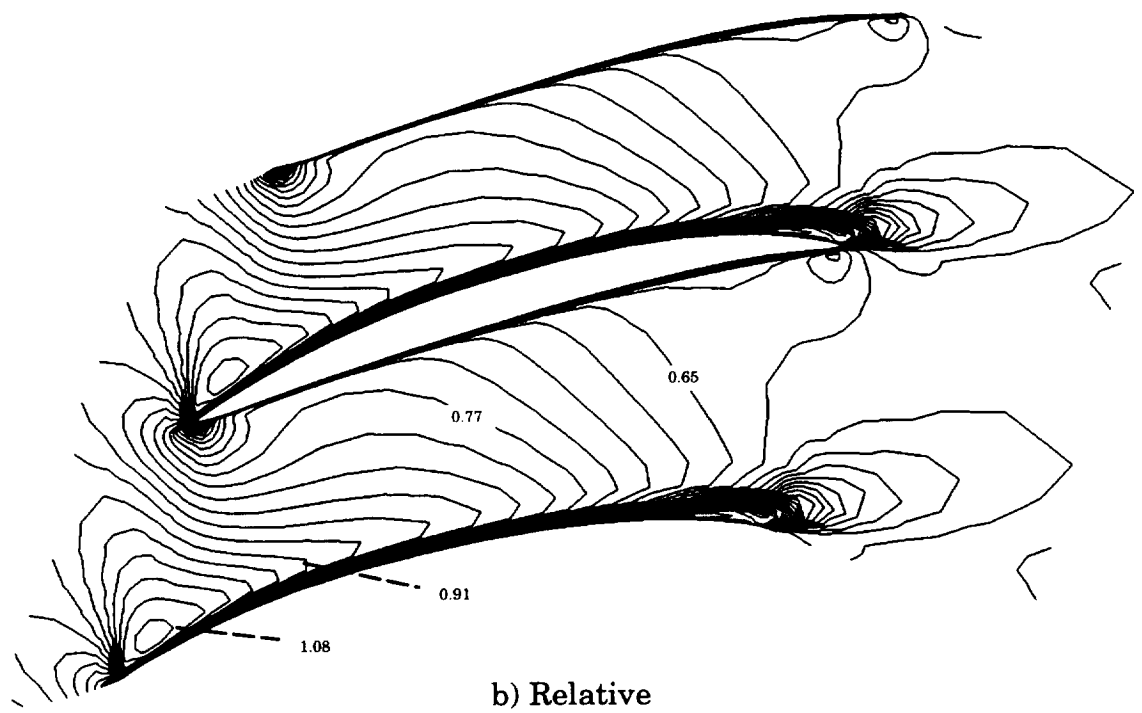
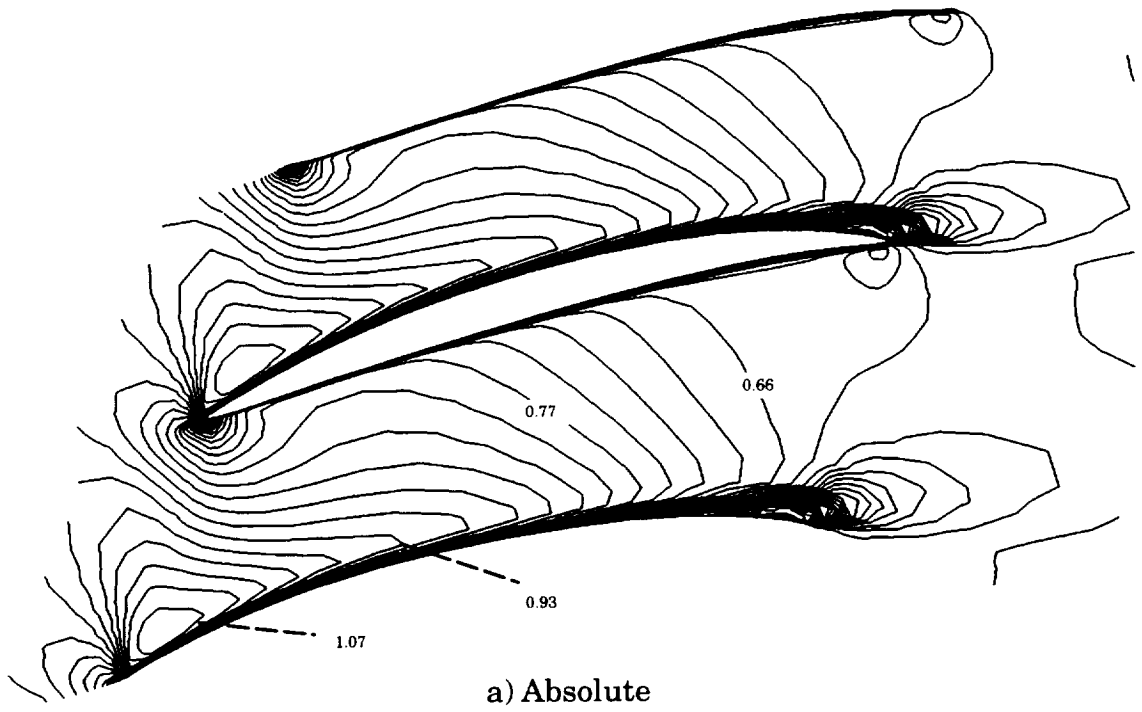


Figure 4.15 Relative Mach No. Contours at 70% Span for Near Peak Efficiency

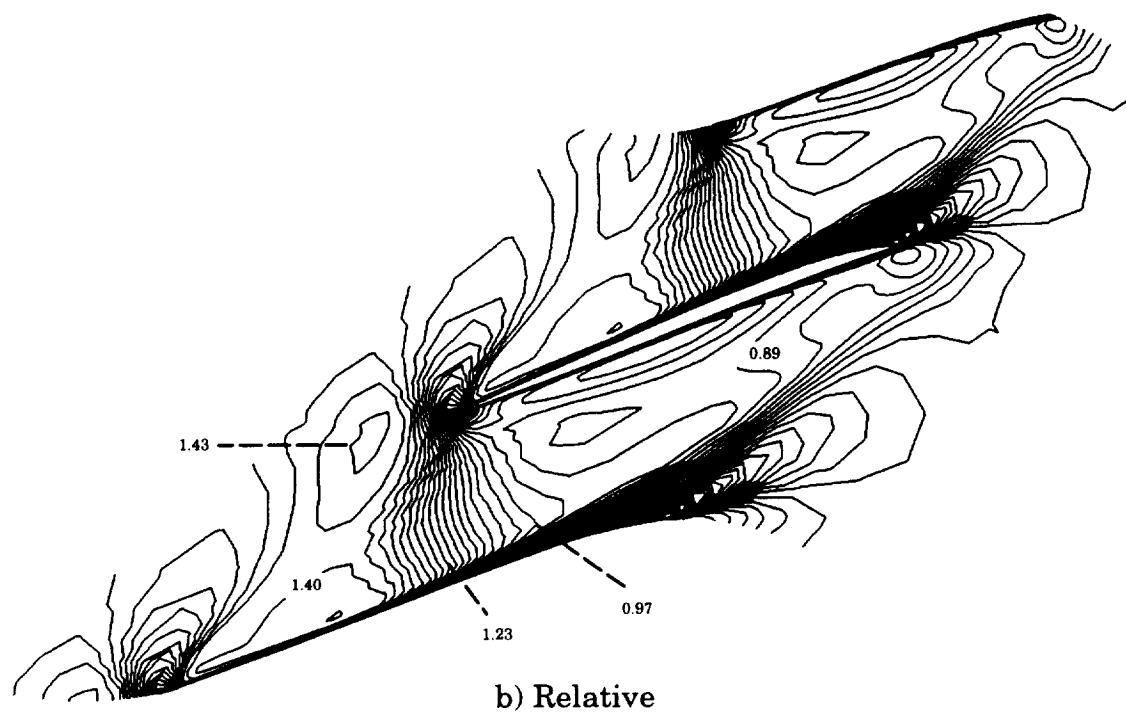
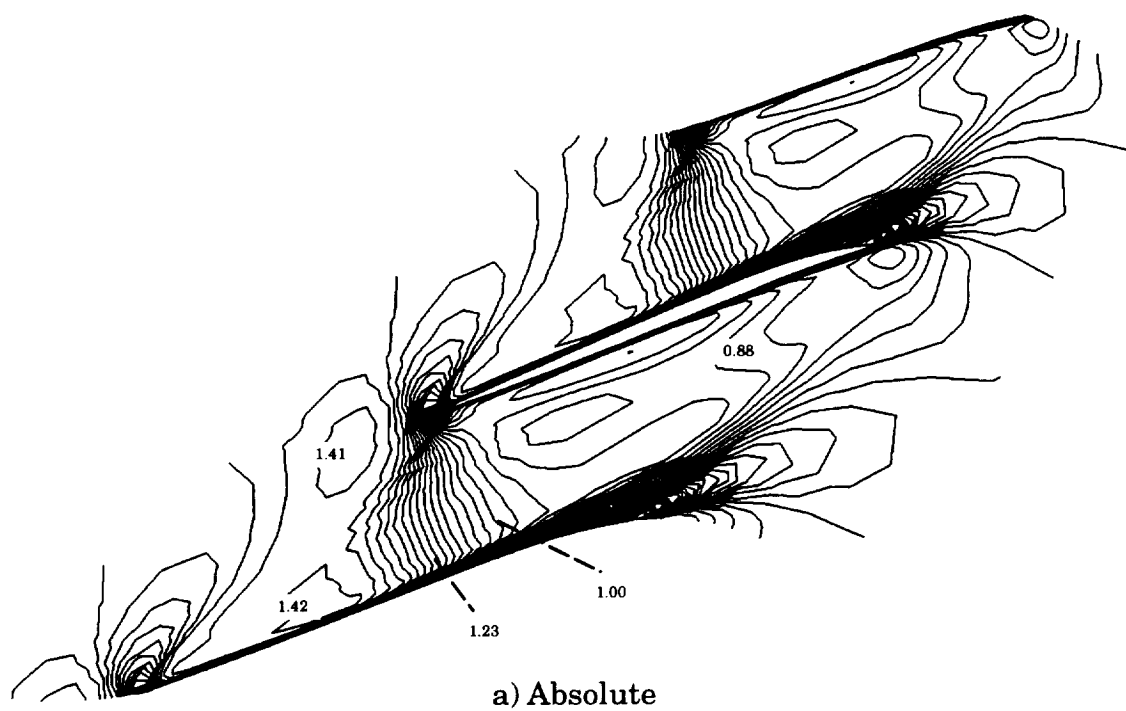


Figure 4.16 Relative Mach No. Contours at 10% Span for Near Stall

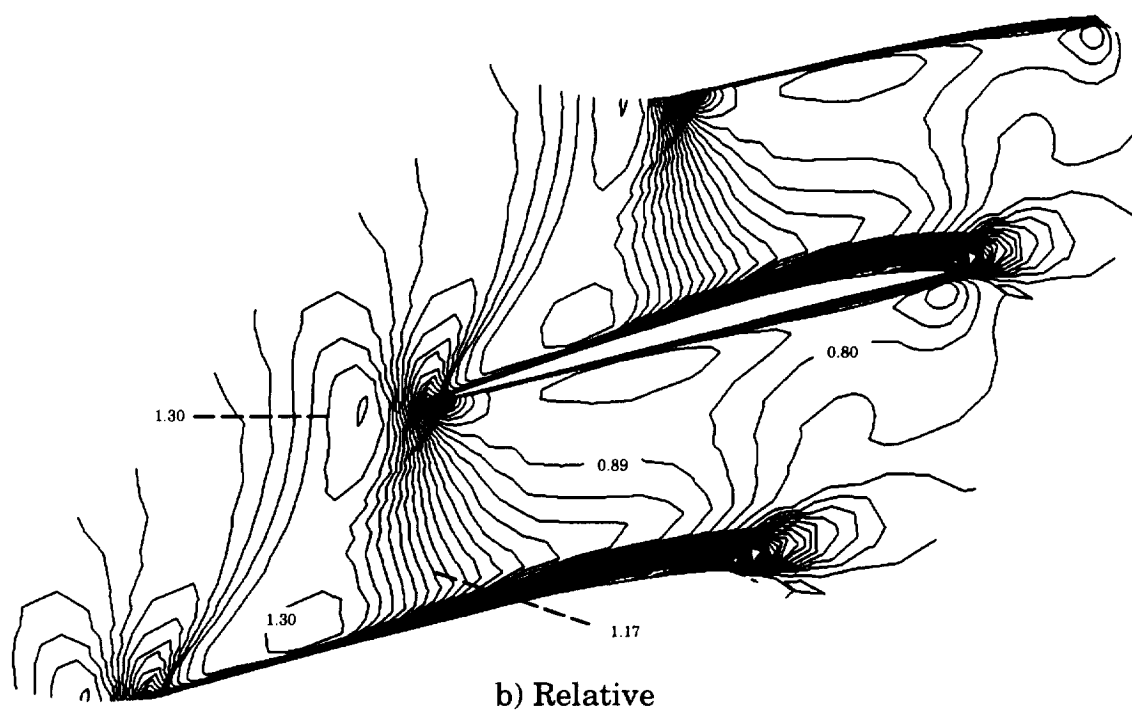
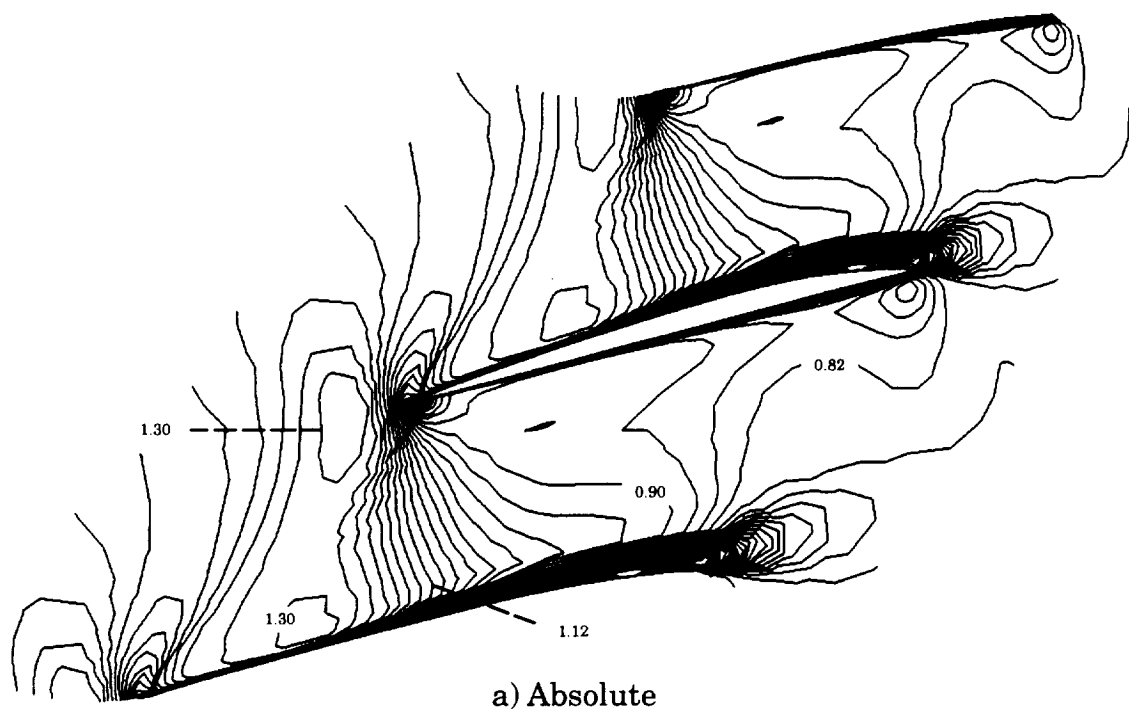


Figure 4.17 Relative Mach No. Contours at 30% Span for Near Stall



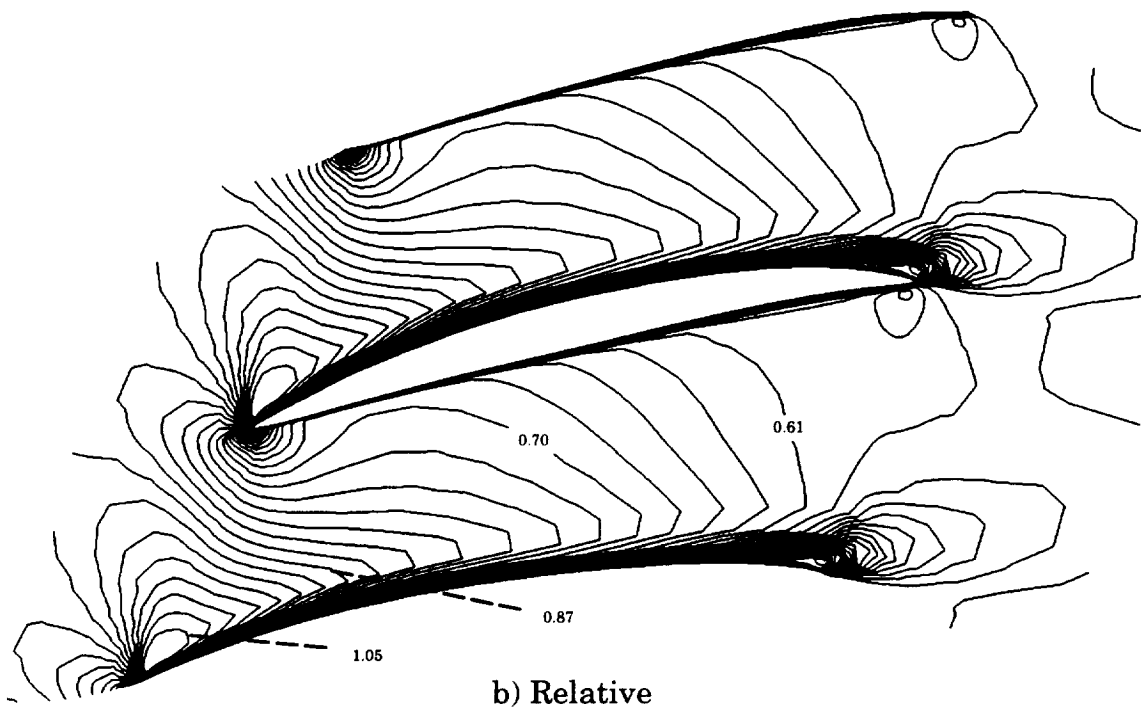
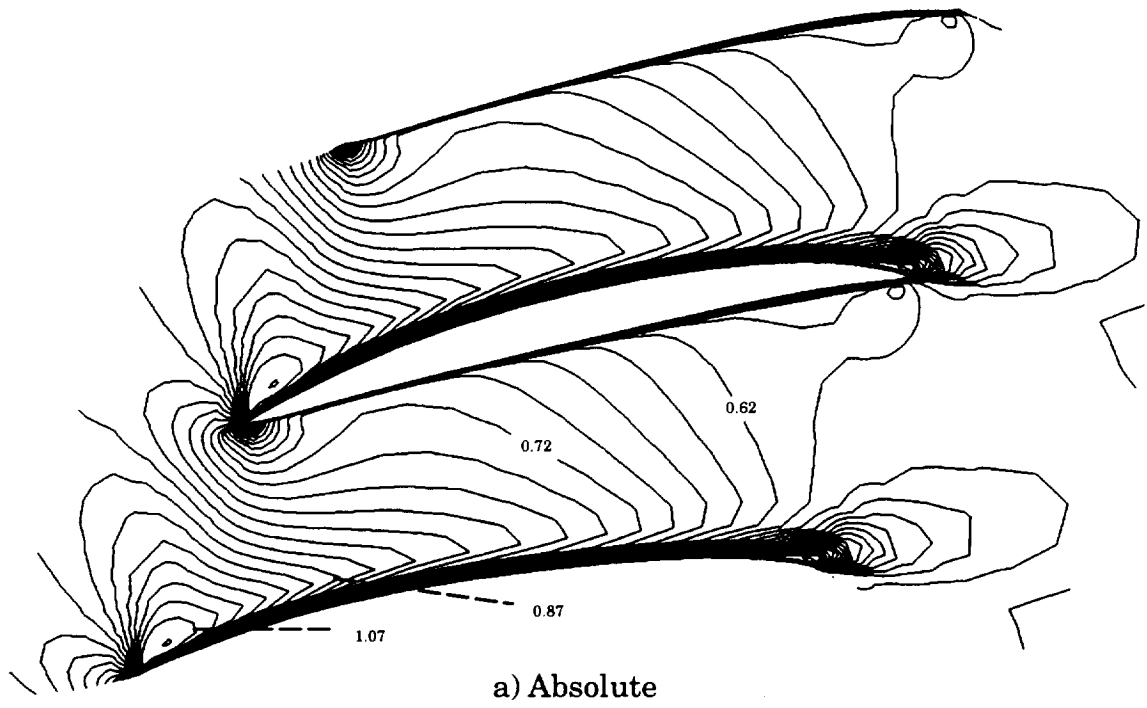


Figure 4.18 Relative Mach No. Contours at 70% Span for Near Stall

## CHAPTER V

### SUMMARY AND CONCLUSIONS

The results presented in Chapter IV amply demonstrated that solving the Navier-Stokes equations in rotating coordinates is a worthwhile exercise and provides a huge advantage in terms of savings in computer time. The savings are due to two main advantages of the rotating frame approach over the inertial frame approach. Since the flow can be considered to be steady in the rotating frame, no Newton sub-iterations are required so that less computing time is required for each time step. This is augmented by the improved stability of the rotating frame code which allows it to handle a far larger CFL than the absolute frame code. This reduces the total number of cycles that are needed to obtain a converged solution. Also the need to move the grid is obviated due to which the metric terms do not need recomputing after each time step. All the above factors contribute to the huge savings in computing time. The speedup in CPU time obtained for the test case in this study was a factor of 16. Moreover, the approach used in this study did not utilize multigrid method or Jacobian freezing. These two factors can contribute to further savings in computing time.

The enhancement in the performance of the code is achieved by making a few minor modifications to the code to incorporate the rotating frame formulation. To summarize, they are the following:

1. Freezing of the grid motion.
2. Calculating the term  $k_t$ , analytically as described in Chapter II.

3. Addition of the source term implicitly in the flux balance.
4. Addition of the source term in the subsonic outflow CVBC which is coupled with the radial equilibrium equation.

The results presented for the test case show that the solution obtained by the relative frame formulation is in very good agreement with the results obtained with the relative frame formulation. The significant improvement in stability is useful for problems with different time scales in turbomachinery computation. Since the rotating frame formulation freezes the frequency associated with the grid rotation, the time scales associated with other frequency (e.g. blade fluttering ) can be used to investigate the unsteady behavior related to that particular time scale. Thus, it can be concluded that this approach is the right direction to take for simulation of flows through turbomachinery, which can be treated as steady state problems in the rotating frame.

Future work will entail implementing the relative frame formulation for a multi-blade row configuration to simulate the flow through a stage. However, this would involve transformation of the dependant variable vector between the fixed and rotating frames before exchanging information between blade rows. Addition of the multigrid method and parallelization of the code are two other areas of future work.

## REFERENCES

- [1] Adamczyk, J.J., "Model Equation for Simulating Flows in Multistage Turbomachinery," ASME Paper No. 85-GT-226, November 1984.
- [2] Chen, J.P., "Unsteady Three-Dimensional Thin-Layer Navier-Stokes Solutions for Turbomachinery in Transonic Flow," Ph. D. Dissertation, Mississippi State University, Mississippi, December 1991.
- [3] Adamczyk, J.J., Celestina, M.L., Beach, T.A., and Barnett, M., "Simulation of Three-Dimensional Viscous Flow Within a Multistage Turbine," ASME Journal of Turbomachinery, Vol. 112, No. 3, July 1990. pp. 370-376.
- [4] Agarwal, R.K., and Deese, J.E., "Euler Calculations for Flowfield of a Helicopter Rotor in Hover," McDonnell Douglas Research Laboratories, MDRL Report 86-10, June 1986.
- [5] Chima, R.V., and Yokota, J.W., "Numerical Analysis of Three-Dimensional Viscous Internal Flows," AIAA Journal, Vol. 28, No. 5, May 1990. pp. 798-806.
- [6] Warsi, Z.U.A., "Fluid Dynamics: Theoretical and Computational Approaches," CRC Press, Inc., Boca Raton, 1993.
- [7] Whitfield, D.L., "Newton-Relaxation Schemes for Nonlinear Hyperbolic Systems," Engineering and Industrial Research Station Report, MSSU-EIRS-ASE-90-3, Mississippi State University, Mississippi, October 1990.
- [8] Janus, J.M., "The Development of a Three-Dimensional Split Flux Vector Euler Solver with Dynamic Grid Applications," M. S. Thesis, Mississippi State University, Mississippi, August 1984. pp. 14-27.
- [9] Whitfield, D.L., "Implicit Upwind Finite Volume Scheme for the Three-Dimensional Euler Equations," Engineering and Industrial Research Station Report, MSSU-EIRS-ASE-85-1, Mississippi State University, Mississippi, September 1985.
- [10] Belk, D.M., "Three-Dimensional Euler Equations Solutions on Dynamic Blocked Grids," Ph. D. Dissertation, Mississippi State University, Mississippi, August 1986.

- [11] Whitfield, D.L., and Taylor, L.K., "Discretized Newton-Relaxation Solution of High Resolution Flux-Difference Split Schemes," AIAA Paper No. 91-1539, June 1991.
- [12] Roe, P.L., "Approximate Riemann Solvers, Parameter Vectors, and Difference Schemes," *Journal of Physics*, Vol. 43, 1981. pp. 357-372.
- [13] Janus, J.M., "Advanced 3-D CFD Algorithm for Turbomachinery," Ph. D. Dissertation, Mississippi State University, Mississippi, May 1989.
- [14] Simpson, L.B., "Unsteady Three-Dimensional Thin-Layer Navier-Stokes Solutions on Dynamic Blocked Grids," Ph. D. Dissertation, Mississippi State University, Mississippi, December 1988.
- [15] Whitfield, D.L., Janus, J.M., and Simpson, L.B., "Implicit Finite Volume High Resolution Wave-Split Scheme for Solving the Unsteady Three-Dimensional Euler and Navier-Stokes Equations on Stationary or Dynamic Grids," Engineering and Industrial Research Station Report, MSSU-EIRS-ASE-88-2, Mississippi State University, Mississippi, February, 1988.
- [16] Baldwin B.S., and Lomax, H., "Thin Layer Approximation and Algebraic Model for Separated Turbulent Flows," AIAA-78-257, January 1978.
- [17] Sreenivas, K., "High Resolution Numerical Simulation of the Linearized Euler Equations in Conservation Law Form," M. S. Thesis, Mississippi State University, Mississippi, July 1993. pp. 30-31.
- [18] Kisielewski, K.M., "A Numerical Investigation of Rain Effects on Lift Using a Three-Dimensional Split Flux Vector Form of the Euler Equations," M. S. Thesis, Mississippi State University, Mississippi, May 1985. pp. 29-36.
- [19] Whitfield, D.L., Swafford, T. W., Janus, J.M., Mulac, R.A., and Belk, D. M., "Three-Dimensional Unsteady Euler Solutions for Propfans and Counter-Rotating Propfans in Transonic Flow," AIAA-87-1197, June 1987.
- [20] Shih, M.H., "TIGER: Turbomachinery Interactive Grid genERation," M.S. Thesis, Mississippi State University, Mississippi, December 1989.

## APPENDIX A

### DERIVATION OF THE VELOCITY OF THE MOVING COORDINATES

It was stated in Chapter II that the vector  $\underline{w}$  can be proven to be negative of the velocity of the moving frame with respect to the stationary frame. The endeavor in this exercise is to prove the above statement. Only the specific case encountered in this study is treated in this exercise. The figure below describes the situation by considering the plane of rotation.

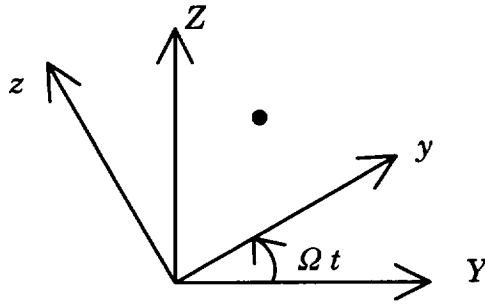


Figure A.1 Plane of Rotation

In the Figure A.1 above,  $Y, Z$  represent the coordinate axes of the stationary inertial frame whereas  $y, z$  represent the axes of the moving frame which is rotating with a constant angular velocity  $\Omega$  about the  $x$  axis, which points out of the paper; so that after time  $t$  the moving axes make an angle of  $\Omega t$  with the respective stationary axes. If one considers a fixed point in space denoted by the dot in the above figure, it will have fixed coordinates in the inertial frame, viz.,  $(X, Y, Z)$ . However, its coordinates in the moving frame, viz.,  $(x, y, z)$  will change over time and can be expressed by the following relations.

$$\begin{aligned} x &= X \\ y &= Y \cos(\Omega t) + Z \sin(\Omega t) \\ z &= Z \cos(\Omega t) - Y \sin(\Omega t) \end{aligned} \tag{A.1}$$

Therefore, the partial time derivatives of the moving coordinates are given by:

$$\frac{\partial x}{\partial t} = 0 \quad (\text{A.2})$$

$$\frac{\partial y}{\partial t} = \Omega [Z \cos(\Omega t) - Y \sin(\Omega t)] = \Omega z \quad (\text{A.3})$$

$$\frac{\partial z}{\partial t} = -\Omega [Y \cos(\Omega t) + Z \sin(\Omega t)] = -\Omega y \quad (\text{A.4})$$

The vector  $\underline{w}$  is defined in equation (2.3) as:

$$\underline{w} = \frac{\partial x^i}{\partial t} \underline{a}_{\sim i} \quad (\text{A.5})$$

According to the coordinate system described in Figure A.1,  $x^1 = x$ ,  $x^2 = y$ ,  $x^3 = z$  and for simplicity let  $\underline{i}$ ,  $\underline{j}$ , and  $\underline{k}$  represent the Cartesian base vectors of the moving frame. Thus,

$$\underline{w} = \frac{\partial x}{\partial t} \underline{i} + \frac{\partial y}{\partial t} \underline{j} + \frac{\partial z}{\partial t} \underline{k} = \Omega z \underline{j} - \Omega y \underline{k} \quad (\text{A.6})$$

The velocity of the moving frame with respect to the inertial frame is given by:

$$\underline{\Omega} \times \underline{r} = \begin{vmatrix} \underline{i} & \underline{j} & \underline{k} \\ \Omega & 0 & 0 \\ x & y & z \end{vmatrix} = -\Omega z \underline{j} + \Omega y \underline{k} \quad (\text{A.7})$$

It can be observed from equations (A.6) and (A.7) that:

$$\underline{w} = -\underline{\Omega} \times \underline{r} \quad (\text{A.8})$$



APPENDIX B  
CURVILINEAR COORDINATE TRANSFORMATION OF THE NAVIER-  
STOKES EQUATIONS

The governing equations in conservation law vector form using non-dimensional variables in rotating Cartesian coordinates is given by:

$$\frac{\partial q}{\partial t} + \frac{\partial f}{\partial x} + \frac{\partial g}{\partial y} + \frac{\partial h}{\partial z} = \frac{\partial f^v}{\partial x} + \frac{\partial g^v}{\partial y} + \frac{\partial h^v}{\partial z} + s \quad (\text{B.1})$$

where the vectors  $q$ ,  $f$ ,  $g$ ,  $h$ ,  $f^v$ ,  $g^v$ ,  $h^v$ , and  $s$  are all defined in equations (2.17)-(2.20). A general nonorthogonal, steady, curvilinear coordinate system is introduced in the  $(x, y, z)$  space as follows:

$$\begin{aligned} \xi &= \xi(x, y, z) \\ \eta &= \eta(x, y, z) \\ \zeta &= \zeta(x, y, z) \\ \tau &= t \end{aligned} \quad (\text{B.2})$$

It should be noted that through equations (B.2) the rotating Cartesian coordinates are transformed to rotating curvilinear coordinates. In other words, the transformation takes place between two coordinate systems within the rotating frame. Using chain rule and writing the result in matrix form yields:

$$\begin{bmatrix} \frac{\partial}{\partial t} \\ \frac{\partial}{\partial x} \\ \frac{\partial}{\partial y} \\ \frac{\partial}{\partial z} \end{bmatrix} = \begin{bmatrix} 1 & 0 & 0 & 0 \\ 0 & \xi_x & \eta_x & \zeta_x \\ 0 & \xi_y & \eta_y & \zeta_y \\ 0 & \xi_z & \eta_z & \zeta_z \end{bmatrix} \begin{bmatrix} \frac{\partial}{\partial \tau} \\ \frac{\partial}{\partial \xi} \\ \frac{\partial}{\partial \eta} \\ \frac{\partial}{\partial \zeta} \end{bmatrix} \quad (\text{B.3})$$

The inverse transformation in matrix form is:

$$\begin{bmatrix} \frac{\partial}{\partial \tau} \\ \frac{\partial}{\partial \xi} \\ \frac{\partial}{\partial \eta} \\ \frac{\partial}{\partial \zeta} \end{bmatrix} = \begin{bmatrix} 1 & 0 & 0 & 0 \\ 0 & x_\xi & y_\xi & z_\xi \\ 0 & x_\eta & y_\eta & z_\eta \\ 0 & x_\zeta & y_\zeta & z_\zeta \end{bmatrix} \begin{bmatrix} \frac{\partial}{\partial t} \\ \frac{\partial}{\partial x} \\ \frac{\partial}{\partial y} \\ \frac{\partial}{\partial z} \end{bmatrix} \quad (\text{B.4})$$

This implies that:

$$\begin{bmatrix} 1 & 0 & 0 & 0 \\ 0 & \xi_x & \eta_x & \zeta_x \\ 0 & \xi_y & \eta_y & \zeta_y \\ 0 & \xi_z & \eta_z & \zeta_z \end{bmatrix} = \begin{bmatrix} 1 & 0 & 0 & 0 \\ 0 & x_\xi & y_\xi & z_\xi \\ 0 & x_\eta & y_\eta & z_\eta \\ 0 & x_\zeta & y_\zeta & z_\zeta \end{bmatrix}^{-1} \quad (\text{B.5})$$

Thus,  $J$ , which is the Jacobian of the inverse transformation, can be written as:

$$J = \begin{vmatrix} 1 & 0 & 0 & 0 \\ 0 & x_\xi & y_\xi & z_\xi \\ 0 & x_\eta & y_\eta & z_\eta \\ 0 & x_\zeta & y_\zeta & z_\zeta \end{vmatrix} = \begin{vmatrix} x_\xi & y_\xi & z_\xi \\ x_\eta & y_\eta & z_\eta \\ x_\zeta & y_\zeta & z_\zeta \end{vmatrix} \quad (\text{B.6})$$

$$= x_\xi(y_\eta z_\zeta - z_\eta y_\zeta) - y_\xi(x_\eta z_\zeta - z_\eta x_\zeta) + z_\xi(x_\eta y_\zeta - y_\eta x_\zeta)$$

The metric terms in equation (B.3) can now be expressed by the following relations:

$$\begin{aligned} \xi_x &= \frac{1}{J}(y_\eta z_\zeta - z_\eta y_\zeta) & \eta_x &= \frac{1}{J}(z_\xi y_\zeta - y_\xi z_\zeta) & \zeta_x &= \frac{1}{J}(y_\xi z_\eta - z_\xi y_\eta) \\ \xi_y &= \frac{1}{J}(z_\eta x_\zeta - x_\eta z_\zeta) & \eta_y &= \frac{1}{J}(x_\xi z_\zeta - z_\xi x_\zeta) & \zeta_y &= \frac{1}{J}(z_\xi x_\eta - x_\xi z_\eta) \\ \xi_z &= \frac{1}{J}(x_\eta y_\zeta - y_\eta x_\zeta) & \eta_z &= \frac{1}{J}(y_\xi x_\zeta - x_\xi y_\zeta) & \zeta_z &= \frac{1}{J}(x_\xi y_\eta - y_\xi x_\eta) \end{aligned} \quad (\text{B.7})$$

The governing equations in curvilinear coordinates, therefore are:

$$\begin{aligned}
& \frac{\partial q}{\partial \tau} + \xi_x \frac{\partial}{\partial \xi} (f - f^\nu) + \eta_x \frac{\partial}{\partial \eta} (f - f^\nu) + \zeta_x \frac{\partial}{\partial \zeta} (f - f^\nu) \\
& + \xi_y \frac{\partial}{\partial \xi} (g - g^\nu) + \eta_y \frac{\partial}{\partial \eta} (g - g^\nu) + \zeta_y \frac{\partial}{\partial \zeta} (g - g^\nu) \\
& + \xi_z \frac{\partial}{\partial \xi} (h - h^\nu) + \eta_z \frac{\partial}{\partial \eta} (h - h^\nu) + \zeta_z \frac{\partial}{\partial \zeta} (h - h^\nu) \\
& = s
\end{aligned} \tag{B.8}$$

Multiplying throughout by  $J$  yields the following:

$$\begin{aligned}
& J \left[ \frac{\partial q}{\partial \tau} + \xi_x \frac{\partial}{\partial \xi} (f - f^\nu) + \eta_x \frac{\partial}{\partial \eta} (f - f^\nu) + \zeta_x \frac{\partial}{\partial \zeta} (f - f^\nu) \right. \\
& + \xi_y \frac{\partial}{\partial \xi} (g - g^\nu) + \eta_y \frac{\partial}{\partial \eta} (g - g^\nu) + \zeta_y \frac{\partial}{\partial \zeta} (g - g^\nu) \\
& + \xi_z \frac{\partial}{\partial \xi} (h - h^\nu) + \eta_z \frac{\partial}{\partial \eta} (h - h^\nu) + \zeta_z \frac{\partial}{\partial \zeta} (h - h^\nu) \left. \right] \\
& = Js
\end{aligned} \tag{B.9}$$

Using the identity:

$$J \xi_x \frac{\partial f}{\partial \xi} = \frac{\partial}{\partial \xi} (J \xi_x f) - f \frac{\partial}{\partial \xi} (J \xi_x) \tag{B.10}$$

the equation (B.9) becomes:

$$\begin{aligned}
& \frac{\partial}{\partial \tau} (Jq) - q \frac{\partial J}{\partial \tau} + \frac{\partial}{\partial \xi} [J(\xi_x f + \xi_y g + \xi_z h)] + \frac{\partial}{\partial \eta} [J(\eta_x f + \eta_y g + \eta_z h)] \\
& + \frac{\partial}{\partial \zeta} [J(\zeta_x f + \zeta_y g + \zeta_z h)] - (f - f^\nu) \left[ \frac{\partial}{\partial \xi} (J \xi_x) + \frac{\partial}{\partial \eta} (J \eta_x) + \frac{\partial}{\partial \zeta} (J \zeta_x) \right] \\
& - (g - g^\nu) \left[ \frac{\partial}{\partial \xi} (J \xi_y) + \frac{\partial}{\partial \eta} (J \eta_y) + \frac{\partial}{\partial \zeta} (J \zeta_y) \right] \\
& - (h - h^\nu) \left[ \frac{\partial}{\partial \xi} (J \xi_z) + \frac{\partial}{\partial \eta} (J \eta_z) + \frac{\partial}{\partial \zeta} (J \zeta_z) \right] \\
& = \frac{\partial}{\partial \xi} [J(\xi_x f^\nu + \xi_y g^\nu + \xi_z h^\nu)] + \frac{\partial}{\partial \eta} [J(\eta_x f^\nu + \eta_y g^\nu + \eta_z h^\nu)] \\
& + \frac{\partial}{\partial \zeta} [J(\zeta_x f^\nu + \zeta_y g^\nu + \zeta_z h^\nu)] + Js
\end{aligned} \tag{B.11}$$

Since the curvilinear transformation is steady:

$$\frac{\partial J}{\partial \tau} = 0 \quad (\text{B.12})$$

Using the expressions for the metric terms defined in equation (B.7) one can write:

$$\begin{aligned} & \frac{\partial}{\partial \xi}(J\xi_z) + \frac{\partial}{\partial \eta}(J\eta_z) + \frac{\partial}{\partial \zeta}(J\zeta_z) \\ &= \frac{\partial}{\partial \xi}(x_\eta y_\zeta) - \frac{\partial}{\partial \xi}(x_\xi y_\eta) + \frac{\partial}{\partial \eta}(x_\zeta y_\xi) - \frac{\partial}{\partial \eta}(x_\xi y_\zeta) + \frac{\partial}{\partial \zeta}(x_\xi y_\eta) - \frac{\partial}{\partial \zeta}(x_\eta y_\xi) \\ &= \frac{\partial y}{\partial \xi} \frac{\partial^2 x}{\partial \xi \partial \eta} + \frac{\partial x}{\partial \eta} \frac{\partial^2 y}{\partial \xi \partial \zeta} - \frac{\partial y}{\partial \eta} \frac{\partial^2 x}{\partial \xi \partial \zeta} - \frac{\partial x}{\partial \zeta} \frac{\partial^2 y}{\partial \xi \partial \eta} + \frac{\partial y}{\partial \xi} \frac{\partial^2 x}{\partial \eta \partial \zeta} + \frac{\partial x}{\partial \zeta} \frac{\partial^2 y}{\partial \eta \partial \xi} \\ & \quad - \frac{\partial y}{\partial \zeta} \frac{\partial^2 x}{\partial \eta \partial \xi} - \frac{\partial x}{\partial \xi} \frac{\partial^2 y}{\partial \eta \partial \zeta} + \frac{\partial y}{\partial \eta} \frac{\partial^2 x}{\partial \zeta \partial \xi} + \frac{\partial x}{\partial \xi} \frac{\partial^2 y}{\partial \zeta \partial \eta} - \frac{\partial y}{\partial \xi} \frac{\partial^2 x}{\partial \zeta \partial \eta} - \frac{\partial x}{\partial \eta} \frac{\partial^2 y}{\partial \zeta \partial \xi} \\ &= 0 \end{aligned} \quad (\text{B.13})$$

Similarly

$$\begin{aligned} & \frac{\partial}{\partial \xi}(J\xi_x) + \frac{\partial}{\partial \eta}(J\eta_x) + \frac{\partial}{\partial \zeta}(J\zeta_x) = 0 \\ & \frac{\partial}{\partial \xi}(J\xi_y) + \frac{\partial}{\partial \eta}(J\eta_y) + \frac{\partial}{\partial \zeta}(J\zeta_y) = 0 \end{aligned} \quad (\text{B.14})$$

Thus, the governing equations in curvilinear coordinates are:

$$\frac{\partial Q}{\partial \tau} + \frac{\partial F}{\partial \xi} + \frac{\partial G}{\partial \eta} + \frac{\partial H}{\partial \zeta} = \frac{\partial F^v}{\partial \xi} + \frac{\partial G^v}{\partial \eta} + \frac{\partial H^v}{\partial \zeta} + S \quad (\text{B.15})$$

where

$$Q = Jq = J \begin{bmatrix} \rho \\ \rho u \\ \rho v \\ \rho w \\ e_t \end{bmatrix} \quad (\text{B.16})$$

$$\begin{aligned}
\bar{K} &= J( k_x f + k_y g + k_z h ) \\
&= J \begin{bmatrix} \rho K' \\ \rho u K' + k_x p \\ \rho v K' + k_y p \\ \rho w K' + k_z p \\ e_t K' + p K \end{bmatrix}, \quad \text{where } K' = k_x u + k_y v + k_z w + k_t \\
&\quad \quad \quad k_t = -k_y \Omega z + k_z \Omega y \\
&\quad \quad \quad K = k_x u + k_y v + k_z w
\end{aligned} \tag{B.17}$$

$$\begin{aligned}
\bar{K}^v &= J( k_x f^v + k_y g^v + k_z h^v ) \\
&= J \begin{bmatrix} 0 \\ T_{kx} \\ T_{ky} \\ T_{kz} \\ Q_k \end{bmatrix}
\end{aligned} \tag{B.18}$$

$$S = J_s = J \begin{bmatrix} 0 \\ 0 \\ -\rho w \Omega \\ \rho v \Omega \\ 0 \end{bmatrix} \tag{B.19}$$

In the above equations (B.17) and (B.18),  $\bar{K} = F, G, H$ ;  $K' = U', V', W'$ ;  $K = U, V, W$ ;  $\bar{K}^v = F^v, G^v, H^v$ ; for  $k = \xi, \eta, \zeta$  respectively. The transformed viscous stress and heat flux terms in equation (B.18) can be expressed in terms of the derivatives with respect to curvilinear coordinates by applying the chain rule to the derivatives appearing in the viscous stress and heat flux terms of the viscous flux vectors in equation (2.19). The transformed viscous stress and heat flux terms are defined in detail in equations (2.39)-(2.41).

**APPENDIX C**  
**CYLINDRICAL COORDINATE FORMULATION**

The Navier-Stokes equations in cylindrical coordinates, in an absolute frame with absolute velocity components using non-dimensional variables can be written as:

$$\frac{\partial \bar{q}}{\partial t} + \frac{\partial \bar{f}}{\partial z} + \frac{\partial \bar{g}}{\partial r} + \frac{\partial \bar{h}}{\partial \theta} = \frac{\partial \bar{f}^j}{\partial z} + \frac{\partial \bar{g}^v}{\partial r} + \frac{\partial \bar{h}^v}{\partial \theta} + \bar{k} \quad (\text{C.1})$$

where

$$\bar{q} = \begin{bmatrix} r\rho \\ r\rho u_z \\ r\rho u_r \\ r^2\rho u_\theta \\ r e_t \end{bmatrix} \quad (\text{C.2})$$

$$\bar{f} = \begin{bmatrix} r\rho u_z \\ r(\rho u_z^2 + p) \\ r\rho u_r u_z \\ r^2\rho u_\theta u_z \\ r\rho H u_z \end{bmatrix}, \quad \bar{g} = \begin{bmatrix} r\rho u_r \\ r\rho u_z u_r \\ r(\rho u_r^2 + p) \\ r^2\rho u_\theta u_r \\ r\rho H u_r \end{bmatrix}, \quad \bar{h} = \begin{bmatrix} \rho u_\theta \\ \rho u_z u_\theta \\ \rho u_r u_\theta \\ r(\rho u_\theta^2 + p) \\ \rho H u_\theta \end{bmatrix} \quad (\text{C.3})$$

$$\bar{f}^j = \begin{bmatrix} 0 \\ r\tau_{zz} \\ r\tau_{rz} \\ r^2\tau_{\theta z} \\ r q_z \end{bmatrix}, \quad \bar{g}^v = \begin{bmatrix} 0 \\ r\tau_{zr} \\ r\tau_{rr} \\ r^2\tau_{\theta r} \\ r q_r \end{bmatrix}, \quad \bar{h}^v = \begin{bmatrix} 0 \\ \tau_{z\theta} \\ \tau_{r\theta} \\ r\tau_{\theta\theta} \\ q_\theta \end{bmatrix} \quad (\text{C.4})$$

$$\bar{k} = \begin{bmatrix} 0 \\ 0 \\ \rho u_\theta^2 + p - \tau_{\theta\theta} \\ 0 \\ 0 \end{bmatrix} \quad (\text{C.5})$$



In the above equations  $u_z$ ,  $u_r$ , and  $u_\theta$  are the axial, radial, and tangential absolute velocity components respectively.  $e_t = \frac{P}{\gamma - 1} + \frac{1}{2}\rho(u_z^2 + u_r^2 + u_\theta^2)$  and

$H = \frac{e_t + P}{\rho}$ . Also,

$$\begin{aligned}
 \tau_{zz} &= \frac{2}{3} \frac{\mu}{\text{Re}} \left[ 2 \frac{\partial u_z}{\partial z} - \frac{\partial u_r}{\partial r} - \frac{1}{r} \frac{\partial u_\theta}{\partial \theta} - \frac{u_r}{r} \right] \\
 \tau_{rr} &= \frac{2}{3} \frac{\mu}{\text{Re}} \left[ 2 \frac{\partial u_r}{\partial r} - \frac{1}{r} \frac{\partial u_\theta}{\partial \theta} - \frac{\partial u_z}{\partial z} - \frac{u_r}{r} \right] \\
 \tau_{\theta\theta} &= \frac{2}{3} \frac{\mu}{\text{Re}} \left[ \frac{2}{r} \frac{\partial u_\theta}{\partial \theta} - \frac{\partial u_z}{\partial z} - \frac{\partial u_r}{\partial r} + 2 \frac{u_r}{r} \right] \\
 \tau_{zr} = \tau_{rz} &= \frac{\mu}{\text{Re}} \left[ \frac{\partial u_z}{\partial r} + \frac{\partial u_r}{\partial z} \right] \\
 \tau_{r\theta} = \tau_{\theta r} &= \frac{\mu}{\text{Re}} \left[ \frac{1}{r} \frac{\partial u_r}{\partial \theta} + \frac{\partial u_\theta}{\partial r} - \frac{u_\theta}{r} \right] \\
 \tau_{\theta z} = \tau_{z\theta} &= \frac{\mu}{\text{Re}} \left[ \frac{\partial u_\theta}{\partial z} + \frac{1}{r} \frac{\partial u_z}{\partial \theta} \right]
 \end{aligned} \tag{C.6}$$

$$\begin{aligned}
 q_z &= \tau_{zz}u_z + \tau_{zr}u_r + \tau_{z\theta}u_\theta + \frac{1}{\text{Re}} \left[ \frac{\mu}{(\gamma - 1) \text{Pr}} \right] \frac{\partial T}{\partial z} \\
 q_r &= \tau_{rz}u_z + \tau_{rr}u_r + \tau_{r\theta}u_\theta + \frac{1}{\text{Re}} \left[ \frac{\mu}{(\gamma - 1) \text{Pr}} \right] \frac{\partial T}{\partial r} \\
 q_\theta &= \tau_{\theta z}u_z + \tau_{\theta r}u_r + \tau_{\theta\theta}u_\theta + \frac{1}{\text{Re}} \left[ \frac{\mu}{(\gamma - 1) \text{Pr}} \right] \frac{1}{r} \frac{\partial T}{\partial \theta}
 \end{aligned} \tag{C.7}$$

For flows in a rotating frame, equation (C.1) can be cast in the relative (rotating) frame by the transformation [3]:

$$\theta_{\text{abs}} = \theta_{\text{rel}} - \Omega t \tag{C.8}$$

where  $\Omega$  is the rotational speed (negative with  $\theta$ ). Introducing equation (C.8) into equation (C.1) yields:

$$\frac{\partial \bar{q}}{\partial t} + \frac{\partial \bar{f}}{\partial z} + \frac{\partial \bar{g}}{\partial r} + \frac{\partial(\bar{h} + \Omega \bar{q})}{\partial \theta} = \frac{\partial \bar{f}^u}{\partial z} + \frac{\partial \bar{g}^u}{\partial r} + \frac{\partial \bar{h}^u}{\partial \theta} + \bar{k} \quad (\text{C.9})$$

The above equation is in cylindrical coordinates but in the rotating frame. However, the velocity components in equation (C.9) are the components of the absolute velocity, the only difference being that the components are now expressed in the relative frame. If one introduces a transformation in the relative frame, from the cylindrical  $(z, r, \theta)$  coordinates to the Cartesian  $(X, Y, Z)$  coordinates which is of the form:

$$\begin{aligned} X &= z \\ Y &= r \cos \theta \\ Z &= r \sin \theta \end{aligned} \quad (\text{C.10})$$

equation (2.16) can be derived by repeating the procedure discussed in Appendix A. Using chain rule and writing the result in matrix form yields:

$$\begin{bmatrix} \frac{\partial}{\partial t} \\ \frac{\partial}{\partial z} \\ \frac{\partial}{\partial r} \\ \frac{\partial}{\partial \theta} \end{bmatrix} = \begin{bmatrix} 1 & 0 & 0 & 0 \\ 0 & 1 & 0 & 0 \\ 0 & 0 & Y_r & Z_r \\ 0 & 0 & Y_\theta & Z_\theta \end{bmatrix} \begin{bmatrix} \frac{\partial}{\partial t} \\ \frac{\partial}{\partial X} \\ \frac{\partial}{\partial Y} \\ \frac{\partial}{\partial Z} \end{bmatrix} \quad (\text{C.11})$$

The inverse transformation in matrix form is:

$$\begin{bmatrix} \frac{\partial}{\partial t} \\ \frac{\partial}{\partial X} \\ \frac{\partial}{\partial Y} \\ \frac{\partial}{\partial Z} \end{bmatrix} = \begin{bmatrix} 1 & 0 & 0 & 0 \\ 0 & 1 & 0 & 0 \\ 0 & 0 & r_Y & r_Z \\ 0 & 0 & \theta_Y & \theta_Z \end{bmatrix} \begin{bmatrix} \frac{\partial}{\partial t} \\ \frac{\partial}{\partial z} \\ \frac{\partial}{\partial r} \\ \frac{\partial}{\partial \theta} \end{bmatrix} \quad (\text{C.12})$$

From equation (C.10) the following results can be derived:

$$\begin{aligned}
Y_r &= \cos \theta, & Y_\theta &= -r \sin \theta, & Z_r &= \sin \theta, & Z_\theta &= r \cos \theta \\
r_Y &= \cos \theta, & r_Z &= \sin \theta, & \theta_Y &= -\frac{\sin \theta}{r}, & \theta_Z &= \frac{\cos \theta}{r}
\end{aligned} \tag{C.13}$$

Thus, the Jacobian of the inverse transformation is given by:

$$J = r_Y \theta_Z - r_Z \theta_Y = \frac{1}{r} \tag{C.14}$$

Also, the following relations hold between the components of the absolute velocity vector in the two coordinate systems

$$\begin{aligned}
u_X &= u = u_z \\
u_Y &= v = u_r \cos \theta - u_\theta \sin \theta \\
u_Z &= w = u_r \sin \theta + u_\theta \cos \theta
\end{aligned} \tag{C.15}$$

Although, in the present context, the above relations give the relation between the components of the absolute velocity, it must be mentioned that they are valid for the components of any vector in the two coordinate systems. Applying the chain rule to equation (C.9) and using the relations derived above, yields the following form of the equations:

$$\frac{\partial q}{\partial t} + \frac{\partial f}{\partial X} + \frac{\partial g}{\partial Y} + \frac{\partial h}{\partial Z} = \frac{\partial f^v}{\partial X} + \frac{\partial g^v}{\partial Y} + \frac{\partial h^v}{\partial Z} + s \tag{C.16}$$

where

$$q = \begin{bmatrix} \rho \\ \rho u \\ \rho v \\ \rho w \\ e_t \end{bmatrix} \tag{C.17}$$

$$f = \begin{bmatrix} \rho u \\ \rho u^2 + p \\ \rho uv \\ \rho uw \\ u(e_t + p) \end{bmatrix}, \quad g = \begin{bmatrix} \rho v - \rho \Omega z \\ \rho vu - \rho u \Omega z \\ \rho v^2 + p - \rho v \Omega z \\ \rho vw - \rho w \Omega z \\ v(e_t + p) - e_t \Omega z \end{bmatrix}, \quad h = \begin{bmatrix} \rho w + \rho \Omega y \\ \rho wu + \rho u \Omega y \\ \rho wv + \rho v \Omega y \\ \rho w^2 + p + \rho w \Omega y \\ w(e_t + p) + e_t \Omega y \end{bmatrix} \quad (\text{C.18})$$

$$f^v = \begin{bmatrix} 0 \\ \tau_{xx} \\ \tau_{xy} \\ \tau_{xz} \\ u\tau_{xx} + v\tau_{xy} + w\tau_{xz} + q_x \end{bmatrix}$$

$$g^v = \begin{bmatrix} 0 \\ \tau_{yx} \\ \tau_{yy} \\ \tau_{yz} \\ u\tau_{yx} + v\tau_{yy} + w\tau_{yz} + q_y \end{bmatrix} \quad (\text{C.19})$$

$$h^v = \begin{bmatrix} 0 \\ \tau_{zx} \\ \tau_{zy} \\ \tau_{zz} \\ u\tau_{zx} + v\tau_{zy} + w\tau_{zz} + q_z \end{bmatrix}$$

$$s = \begin{bmatrix} 0 \\ 0 \\ -\rho w \Omega \\ \rho v \Omega \\ 0 \end{bmatrix} \quad (\text{C.20})$$

It can be observed from the above equations (C.17)-(C.20) that the equations in Cartesian coordinates derived via the cylindrical coordinates are identical to equation (2.16).